Thesis for the degree of Doctor of Philosophy

Plasma Oscillations in Holographic Quantum Matter

Marcus Tornsö

Department of Physics
Chalmers University of Technology
Gothenburg, Sweden, 2021

Plasma Oscillations in Holographic Quantum Matter
Marcus Tornsö
ISBN 978-91-7905-525-7

Doktorsavhandlingar vid Chalmers tekniska högskola
Ny serie nr 4992
ISSN 0346-718X

Department of Physics
Chalmers University of Technology
SE–412 96 Gothenburg
Sweden
Telephone +46 (0)31-772 1000

Chalmers Reproservice
Gothenburg, Sweden, 2021

Plasma Oscillations in Holographic Quantum Matter
MARCUS TORNSÖ
Department of Physics
Chalmers University of Technology

Abstract

In this thesis we explore strongly correlated matter in the framework of holographic duality. Specifically, we examine the quasinormal modes of such systems, and we extend the current framework to efficiently and naturally cover plasmons and other collective modes that may be found within strongly correlated matter.

The interest in strongly correlated matter is motivated by the presence of a "strange metal" phase both in high temperature superconductors and in near charge neutral graphene, both being materials of immense scientific interest. The strange metal phase is a phase characterized by the absence of quasi-particles. This implies that conventional methods, such as perturbation theory in quantum field theory and Monte Carlo methods fall short of being able to describe the dynamics. Perhaps surprisingly, string theory provides a novel method, capable of precisely describing such systems - the holographic duality.

With the holographic duality, strongly coupled matter is mapped onto a weakly coupled gravity theory in one additional dimension, allowing for a conventional treatment of the dual system.

In this thesis, we extend the existing framework to also describe polarizing media. This is explicitly done in the form of new boundary conditions on the holographic dual, which deviate from previous holographic studies, and we contrast the quasinormal modes previously studied with the emergent collective modes we find for some studied models. We find new results, as well as confirm the predictions of less general models in their respective regions of validity and pave the way for more complex future models.

Keywords: holography, plasmonics, strong coupling, graphene, quasinormal modes, gauge/gravity duality, strongly correlated media

Publications

This thesis is based on the following publications:

I. **Holographic plasmons**
U. Gran, M. Tornsö, T. Zingg
Journal of High Energy Physics 11, 176 (2018).

II. **Plasmons in holographic graphene**
U. Gran, M. Tornsö, T. Zingg
SciPost Phys. 8, 93 (2020).

III. **Exotic Holographic Dispersion**
U. Gran, M. Tornsö, T. Zingg
Journal of High Energy Physics 2, 32 (2019).

IV. **Holographic Response of Electron Clouds**
U. Gran, M. Tornsö, T. Zingg
Journal of High Energy Physics 3, 19 (2019).

V. **Holographic Plasmon Relaxation with and without Broken Translations**
M. Baggioli, U. Gran, A. Jimenez Alba, M. Tornsö, T. Zingg
Journal of High Energy Physics 9, 13 (2019).

VI. **Transverse Collective Modes in Interacting Holographic Plasmas**
M. Baggioli, U. Gran, M. Tornsö
Journal of High Energy Physics 4, 106 (2020).

VII. **Collective modes of polarizable holographic media in magnetic fields**
M. Baggioli, U. Gran, M. Tornsö
Journal of High Energy Physics 6, 14 (2021).

VIII. **Holographic fundamental matter in multilayered media**
U. Gran, N. Jokela, D. Musso, A. Vásques Ramallo, M. Tornsö
Journal of High Energy Physics 12, 38 (2019).

Statement of contribution

For paper I, I, the author of this thesis, was a significant contributor to working out the plasmon condition in terms of holographically available quantities, the key component in extending the holographic framework. I was also the main contributor in adapting the plasmon condition to the different settings of subsequent work, II-VII. Additionally, I was the one to observe and highlight the exotic phenomena found resulting in paper III. For papers I-VII I carried out the analytical computations as well as developed the computer model and all the numerical tools used, produced the data for all different parameter setups considered, and most graphical presentations. I was also a significant contributor to the interpretation of said data, discussion thereof, and writing of the following articles.

For paper VIII my contribution was to carry out all analytical calculations, which were all carried out by multiple authors. That is, I was either double checking calculations by other collaborators, or making calculations to be double checked by other collaborator. I also contributed to the writing of the resulting article.

All authors are listed in alphabetical order rather than by weight of contribution.

Acknowledgments

First and foremost, I want to thank my supervisor Ulf Gran, without whom this project would not have been possible. I would also like to thank my assistant supervisors Bengt E.W. Nilsson and Henrik Johannesson for their support.

Further, I would like to thank Tobias Wenger and Andreas Isaksson for many insightful discussions, and my collaborators Tobias Zingg, Niko Jokela, Alfonso Vásquez Ramallo, Daniele Musso, Matteo Baggioli and Amadeo Jimenez Alba for their intellectual contributions to my knowledge.

I am also grateful to the Royal Swedish Academy of Sciences, Wilhelm & Martina Lundgrens Vetenskapsfond and The Lars Hierta Memorial Foundation for the travel grants that have allowed me to attend several conferences during my studies.

My thanks to the Division of Subatomic, High Energy and Plasma Physics for taking me on, and helping me along the way.

Lastly, for their persistent support, I thank my family and most importantly my wife; you have my deepest gratitude and eternal love, Amanda.

Marcus Tornsö, 2021

Contents

Chapter 1

Introduction

What is simple is always wrong. What is not is unusable. - Paul Valéry

This quote encapsulates the very essence of the problem this thesis concerns. In the study of extreme quantum matter, where quantum mechanical effects are significant between countless particles and long length scales, traditional microscopic descriptions fall short when predicting macroscopic behaviour. However, new approximations can be made in surprising ways, resulting in a unification between this smallest physics, and the largest – in the form of black holes. This effective description most certainly is not correct on all levels – just like any good *model* – but it works on the macroscopic levels of interest.

In this thesis, we build upon previous thesis work by the author [1] and explore strongly correlated matter in the framework of holographic duality. Specifically, the quasinormal modes of such systems will be examined, and we will extend the current framework to efficiently and naturally cover plasmons and other collective modes that may be found within. Matter of particular interest are graphene and cuprate superconductors, exciting materials for scientific study in their own right, but here specifically as they exhibit strong coupling at certain temperatures and doping.

The considerable attention strongly coupled media has attracted by the scientific community is justified by the immense potential these materials hold, with high-temperature superconductors arguably being the most important ones. Conventional superconductivity was discovered as early as 1911, by Onnes [2]. This is a property that many materials possess when cooled to extremely low temperatures. A superconducting material, as the name suggests, conducts electrical currents perfectly, and as a direct consequence can freely counteract magnetic fields. There are many interesting and less obvious consequences from this, some superconductors (called type-I) completely expel magnetic fields, weheras others (type-II) exhibit flux pinning. This means that the strength of the magnetic field cannot change, implying that magnets can be locked at fixed distances from the supercon-

ductors, in a stable quantum levitation. Without any energy lost for internal electrical currents, the material responds to any change in magnetic field by essentially acting as a repulsive – or attractive – electromagnet to prevent any change in magnetic field which would be induced by a movement of the magnet, effectively locking it at a fixed distance. Lossless transport of electricity, and frictionless transport of wares are immediate, revolutionary applications of such materials, but their uses encompass also more technical purposes, such as strong electromagnets and devices for quantum computing.

A theory for conventional superconductivity was developed by Bardeen, Cooper and Schrieffer in the 1950s [3], a theory that is now called BCS-theory and for which they were awarded the Nobel prize in 1972. The central point of their theory is that electrons in these materials can pair up into *Cooper pairs*, which are composite bosons, unlike their constituent electrons which are fermions. As bosons, multiple Cooper pairs can occupy the same quantum state, which is exactly what happens at low temperatures, and brings the degenerate ground state that provides superconductivity, see figure 1.1. The Cooper pairs are however delicate, and are destroyed at

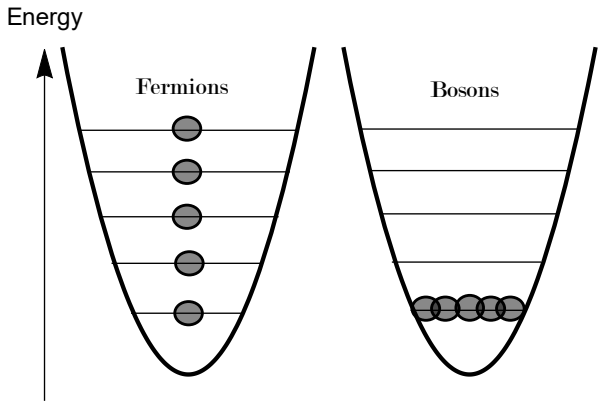

Figure 1.1: Ground states for a system of fermions and a system of bosons. The degeneracy of the bosonic system results in, among other things, a considerably lower energy.

high temperatures. They can therefore only exist at very low temperature, and the theory suggested it was highly improbable that superconductivity could be observed outside of cryogenics laboratories. Nevertheless, Bednorz and Müller discovered the existence of high-temperature superconductors in 1986 [4] and for this remarkable discovery were awarded the Nobel prize already the following year. As of today, compounds have been found that have critical temperatures of, i.e. are superconductive up to, 138K, under normal pressure. Whereas, this may still seem far from the dream of room-temperature ($\sim$ 290K) superconductivity, it is worth noting that it is still on

the same order of magnitude, and our understanding of high-temperature superconductors is still very scarce. Additionally, these temperatures are high enough to allow for superconductivity with liquid nitrogen cooling, substantially simpler to accomplish than the cryogenics needed for conventional superconductors.

High-temperature superconductors are therefore very promising, but has so far eluded a proper theoretical description. The most important feature to understand is the critical temperature, the temperature at which, when cooled to, they become superconducting. A natural part of this puzzle, is to also understand what is on the other side of this point: the so-called "strange metal". This fittingly named phase is characterized by the absence of long-lived quasiparticles, and is ruled by strong Coulomb interactions. Ordinary metals are typically also strongly coupled, but they can be described as Fermi-liquids including quasiparticles, which is why the existing treatment of metals has been as successful as it has. This is not the case for strange metals, and the absence of long-lived quasiparticles makes the use of conventional tools such as perturbation theory or Monte-Carlo methods impossible. There is thus a need for other, alternative models to describe these materials, and holography is one of very few possibilities that fits the bill.

That strange metals are essentially an uncharted territory of physics is another very natural reason to want to study them.

In a similar vein, there has been an enormous interest in studying graphene, since Geim and Novoselov discovered it in 2004 and were awarded a Nobel prize in 2010. Graphene is a material that is as two-dimensional as anything can be, only a single atom thick, and has many very extreme properties related to that. Incredible strength, large conductivities, optical transparency are some generic ones, with many more specifics, such as e.g. its electrons behaving more or less as massless particles. Graphene's immense potential has led to many aspiring and extensive research project, especially notable being the EU's Graphene Flagship project.

And as if that wasn't enough, under certain conditions, bilayer graphene can both be superconducting and a strange metal. Near charge neutrality, graphene behaves strongly coupled, and even though this was predicted theoretically, the phase itself is difficult to model more exactly. Once more the holographic approach is motivated, but now for another, very different type of material.

When studying strange metals, there are many properties that could be of interest to describe, and many of them are accessible with holographic tools. In superconductors, the most important properties originate from how charged particles interact with each other, and thus it was a natural choice for this thesis to focus on the dynamical charge response of holographic systems. Specifically, we have considered the collective excitations of such systems, with one particularly important one in mind: the "plasmon" mode.

The plasmon is the most easily excited collective mode, and are present in all conducting matter. As the name implies, they are quanta of plasma oscillations, and for our purposes, may need two clarifications.

Firstly, a proper plasma is a state of matter that is essentially a gas of ions. As such it is typically found in superheated matter, where the thermal energy is large enough to separate electrons from the nuclei. However, in metals, there are electrons that are free to move inside a lattice of positively charged ions, and as such the electrons behave much like a plasma (in a positively charged background) without any large temperatures. It is the oscillations in this type of plasma we will consider in our studies of plasmons.

Secondly, the qualifier of a quanta is of little use in strange metals, as they have no quasiparticle description. Instead, we will use the natural extension and refer to the lowest, propagating and self-sourced excitations of a plasma as plasmons. In limits where these can be considered long-lived, conventional plasmons are quanta of these.

There are many reasons to study plasmons; they are a natural phenomenon with many practical applications due to their particular properties. Their close relationship to both light and electrical currents often make them ideal when it comes to miniaturization of circuits [5, 6] or making ultrafast and sensitive detectors [7]. *Plasmonics*, much like photonics, is a scientific field in its own right, and concerns the utilization of plasmons in technology. One particular property of interest for plasmons is that they exhibit a strong wave localization compared to that of ordinary light, i.e. plasmonic waves are more compressed than ordinary electromagnetic waves. A material that exhibits a particularly strong wave localization is graphene [8], which not only makes it an excellent candidate for various applications within plasmonics, but also gives another reason to study strongly coupled plasmonics in this thesis. Since graphene is effectively two-dimensional, there is reason to study strongly coupled plasmons not only in three dimensions, but also two, both of which have been the focus of our research.

This thesis is structured as follows. In chapter 2, an introduction to plasmons (and other types of electromagnetic modes) from Maxwell theory is given, as well as the predictions from a few common models at weak coupling. Chapter 3 gives a brief introduction to strange metals, the quantum matter that is the target for this thesis. In chapter 4, the holographic duality is presented in its conventional form, as well as the simple and established anti-de Sitter Reissner-Nordström model. We then start from this conventional model and step by step expand upon it in chapter 5, which encompasses seven articles from the publication list. Lastly, the thesis finishes off with some future directions of this research that I find particularly interesting and promising, with some current and preliminary highlights. The chapters are designed in such a way to allow an interested reader to start reading any chapter, and within each chapter the content grows increasingly more technical the further the reader gets.

Chapter 2

Plasmons

Plasmons are per definition excitations of a plasma. A plasma is much like a gas, but rather than having a composition of neutral atoms or molecules, a plasma is made of charged ions. As such the forces between individual particles are much stronger than compared to ordinary gasses. Plasma is often considered the fourth phase of matter, after solid, liquid and gas, and it is typically in that order they transition into each other with increasing temperature or, correspondingly, decreasing pressure.

However, this is not the type of plasma we primarily aim to describe here. We instead consider metals, i.e. solids, but where a rigid crystalline lattice of positively charged nuclei is filled with more or less bound negatively charged electrons. If the electrons are not all bound by the nuclei, then one can consider the metal as a background of positively charged ions, in which a density of electrons is free to move, very much like a plasma. The movement of the electrons is typically slow, and as they interact with strong Coulomb forces, their behaviour is more like that of a liquid. Certain properties can be well described by traditional hydrodynamic methods. It is therefore not uncommon that the electron plasma, inside a solid, is referred to as a gas or a liquid as well. The nomenclature is far from perfect.

Plasmons are quanta of wavelike excitations in this plasma, much like sound waves. However, compared to sound waves they have a more complicated frequency dependence, with several qualitatively different effects, such as e.g. highly frequency dependent velocities.

The most fundamental plasma excitation is typically only referred to as plasma oscillation. Here, the plasma simply oscillates back and forth without propagating, at a fixed frequency determined by the system, the so-called plasma frequency, ω_p. This can actually be derived rather straightforwardly, one way is shown in section 2.3.1. These excitations can also propagate if one introduces a wavelength and they are also commonly referred to as Langmuir waves.

There are multiple types of plasmons. One way to separate them is

whether the charged particles move in the same direction as the wave (longitudinal) or in a perpendicular direction (transversal). There are also localized plasmons (e.g. confined to nanoparticles). There is also a distinction between bulk and surface plasmons. Bulk plasmons can roughly be categorized as living in a medium that is homogeneous (or even isotropic) - i.e. there is no significant difference in different points. Surface plasmons do not fulfill that criteria. A surface plasmon lives on the interface between two media (e.g. the surface on a metal, the plasmon has metal on one side, air on the other). These are also sometimes known as polaritons (implying they are a hybridization of a charge wave in the medium and a field wave outside). It should also be mentioned that arguably surface plasmons could be separated into two categories itself, interface plasmons – where the plasmons essentially live on the boundary of a material, with another medium next to it, and sheet or 2D plasmons – where the plasmons effectively live in a thin sheet, with different media on both sides. In the literature, the latter is often discussed in the context of 2D electron gasses (2DEG), but some sheets, e.g. graphene, have extreme properties that often exclude them from that category. Specifically, graphene can have a strong coupling and the free electrons are then better described as a fluid than a gas. This is often referred to as the Dirac fluid phase.

In this thesis, we focus mainly on longitudinal and transverse bulk plasmons and longitudinal 2D plasmons.

2.1 History

While plasmons are relatively difficult to describe theoretically, and were first so in the 20th century, they have unknowingly been used for centuries, back to as early as 400 AD. Phenomenologically, surface plasmons are easily excited by incident light on smooth metallic surfaces where they live for a short while, before they decay, and re-emit the light. Some wavelengths are more difficult to absorb than others, which means there will be a coloring effect. This effect has for instance been used by the Romans to dye cups and later by adding small metallic beads to stain glass windows to different colors [9, 10]. As the plasmons move along the surface of the metallic beads and re-emit the light in a different direction, this method of colouring glass has the neat effect that transmitted and reflected light has different colours, meaning the colours change depending on the position of the light source relative to the viewer.

The underlying physics was of course unknown then. Not until Maxwell compiled his famous equations in 1861 were plasmons even possible to describe, and it wasn't until the 1920s they were "discovered" by Langmuir and Tonks [11]. In 1956 they were properly described in their quantized form by Pines [12].

Today, plasmons are used extensively, enough so for "plasmonics" to be a proper field in itself [13, 14]. They are used in spectroscopy for signal enhancing (e.g. surface enhanced Raman spectroscopy, SERS) and in extremely sensitive detection of nanoparticles (e.g. detection of flammable gasses in cars and factories).

A lot of the interest in plasmons comes from the large wave localization they bring, allowing for the miniaturization of circuits and also localization of energy, which brings the great enhancement in SERS.

2.2 Properties

Plasmons can be well described with classical electromagnetism, e.g. [15], where the interaction between charged particles is governed by Maxwell's equations,

$$\nabla \cdot \boldsymbol{E} = \frac{\rho}{\epsilon_0}\,, \tag{2.1}$$

$$\nabla \times \boldsymbol{B} - \frac{1}{c^2}\frac{\partial \boldsymbol{E}}{\partial t} = \mu_0\, \boldsymbol{J}\,, \tag{2.2}$$

$$\nabla \cdot \boldsymbol{B} = 0\,, \tag{2.3}$$

$$\nabla \times \boldsymbol{E} + \frac{\partial \boldsymbol{B}}{\partial t} = 0\,. \tag{2.4}$$

Here $\boldsymbol{E}$ is the electric field, $\boldsymbol{B}$ is the magnetic field, ρ is the charge density and $\boldsymbol{J}$ is the current density. ϵ_0 and μ_0 are the permittivity and permeability of vacuum respectively. These equations were found individually, and as such have individual names with which they are sometimes referred to as: (2.1) is Gauss' law, (2.2) is Ampère's law, (2.3) is Gauss' law for for magnetism and (2.4) is Faraday's law. From these many familiar relations can be derived, most notably the continuity equation,

$$0 = \nabla \cdot \boldsymbol{J} + \frac{\partial \rho}{\partial t}\,, \tag{2.5}$$

equating the flow of charges to the change in charge density at any point, and thus the charge of a system is preserved.

It is often convenient to separate the macroscopic contributions from the response of a medium and the applied fields from the total fields $\boldsymbol{E}$ and $\boldsymbol{M}$. We introduce the polarization $\boldsymbol{P}$ of the medium as the response of an applied displacement field $\boldsymbol{D}$, the magnetization $\boldsymbol{M}$ of the medium as the response to an applied magnetizing field $\boldsymbol{H}$. It should be mentioned that this viewpoint is generally useful, although there are situations where the polarization and magnetization are not the response to external fields, e.g. electrets and ferromagnets. We also separate the different contributions to the densities, into an induced charge density $\langle\rho\rangle$, an induced current

density $\langle \boldsymbol{J} \rangle$, an applied external charge ρ_{ext} and an applied external current $\boldsymbol{J}_{ext}$. Specifically, these are

$$\boldsymbol{E} = \frac{1}{\epsilon_0} \left(\boldsymbol{D} - \boldsymbol{P} \right) , \tag{2.6}$$

$$\boldsymbol{B} = \mu_0 \left(\boldsymbol{H} + \boldsymbol{M} \right) , \tag{2.7}$$

$$\rho = \rho_{ext} + \langle \rho \rangle , \tag{2.8}$$

$$\boldsymbol{J} = \boldsymbol{J}_{ext} + \langle \boldsymbol{J} \rangle . \tag{2.9}$$

Where the induced charge and current densities are often difficult to keep track of as that would require a proper microscopic description of the materials. The external ones are however very natural, allowing us to write Maxwell's equations in a convenient macroscopic way, turning (2.1) and (2.2) into

$$\nabla \cdot \boldsymbol{D} = \rho_{ext} , \tag{2.10}$$

$$\nabla \times \boldsymbol{H} - \frac{\partial \boldsymbol{D}}{\partial t} = \boldsymbol{J}_{ext} . \tag{2.11}$$

Similarly, one can formulate continuity equations for induced and external charges and currents as well.

Furthermore, by defining the dielectric function, ϵ, by

$$\boldsymbol{D} = \epsilon \boldsymbol{E} , \tag{2.12}$$

the conductivity, σ, by

$$\boldsymbol{J} = \sigma \boldsymbol{E} , \tag{2.13}$$

one can write the solutions of these equations in a more explicit manner. Note that the quantities ϵ and σ in general are matrices. These matrices account for measurable and important quantities of any medium, furthermore they are linked to each other by the equations above. They can also depend non-trivially on the field strength $\boldsymbol{E}$ itself, effectively making the material inhomogeneous and time-dependent for varying fields. However, in general, a system can be treated in linear response, assuming small fields and thus negligible higher order contributions to σ and ϵ.

With these definitions, one can extract a relation between σ and ϵ. Differentiating the difference between (2.10) and (2.1) with respect to time, substituting $\boldsymbol{D}$ as in (2.12) and ρ using the continuity equation and $\boldsymbol{J}$ as in 2.9 and (2.13), one finds

$$\frac{d}{dt} \left[\nabla \cdot \left(\epsilon_0 - \epsilon \right) \boldsymbol{E} \right] = -\nabla \cdot \sigma \boldsymbol{E} . \tag{2.14}$$

In linear response it becomes natural to assume the medium to be homogeneous (unchanging in space) and time-independent. A common situation

is also to study isotropic media, in which the dielectric function and conductivity are the same in all directions. The derivatives then commute with σ and ϵ and we can simply move them to the fields,

$$\left[(\epsilon_0 - \epsilon)\frac{d}{dt} + \sigma\right]\nabla \cdot \boldsymbol{E} = 0\,. \tag{2.15}$$

That is, when $\nabla \cdot \boldsymbol{E} \neq 0$, which is the case for longitudinal modes, the expression in brackets has to be zero. For individual frequencies, i.e. the time dependence of $\boldsymbol{E}$ is proportional to $e^{-i\omega t}$, this means

$$\epsilon = \epsilon_0 + i\frac{\sigma}{\omega}\,. \tag{2.16}$$

It is worth pointing out here that defining the electric susceptibility χ_P as

$$\boldsymbol{P} = \chi_P \boldsymbol{E}\,, \tag{2.17}$$

(2.16) simply yields

$$\chi_P = i\frac{\sigma}{\omega}\,. \tag{2.18}$$

2.2.1 The plasmon condition

As previously stated, there are multiple types of excitations of a system. The importance of external charges of currents is manifest in equations (2.10)-(2.11). The excitations we refer to as plasmons are self-sourced excitations, i.e. they are solutions to Maxwell's equations in the absence of external influence. Equation (2.10) then implies that

$$\epsilon = 0\,, \tag{2.19}$$

which is what we refer to as the *plasmon condition*, or that the solution is trivial, i.e. $\boldsymbol{E} = \langle \boldsymbol{J} \rangle = 0$.

It is worth mentioning that plasmons commonly refer to a specific subset of the solutions to this condition that are propagating, or even only the lowest energy solution of these. In fact, since the absence of external charges is something that is common for collective excitations, we refer to the solutions as collective modes, however, in general it's the lowest propagating collective mode that is of interest, i.e. the plasmon mode.

Another common type of mode to describe are the quasinormal modes (QNM). These are poles of the conductivity, or the screened density-density correlator

$$\chi_{sc} = \langle \rho\, \rho \rangle = \frac{k^2}{i\omega}\sigma\,, \tag{2.20}$$

whereas collective modes are the poles of the full density-density correlator [16],

$$\chi = \chi_{sc}/\epsilon\,. \tag{2.21}$$

QNMs correspond to solutions where you can have an induced current, even without an electric field, with a driving external current. They are interesting in their own right, and are closely related to, but sometimes qualitatively different than, collective modes.

2.2.2 In terms of potentials

The governing equations are commonly solved in terms of electromagnetic vector potentials, i.e.

$$\boldsymbol{E} = -\frac{\partial \boldsymbol{A}}{\partial t} - \nabla\phi\,. \tag{2.22}$$

Looking at equation (2.2) in the absence of a magnetic field we find

$$-\epsilon_0 \dot{\boldsymbol{E}} = \langle \boldsymbol{J} \rangle\,. \tag{2.23}$$

Without loss of generality, choosing the momentum to be in the x-direction and choosing $\phi = 0$ gauge, this equation can be written as

$$\omega^2 A_x + J_x = 0\,. \tag{2.24}$$

Similarly, in Coulomb gauge (with $\boldsymbol{A} = 0$), it can be written

$$k^2\phi - \rho = 0\,. \tag{2.25}$$

For quasinormal modes, $\boldsymbol{J} = \sigma\boldsymbol{E} = 0$ and thus the condition simply becomes

$$\phi = 0\,, \qquad A_x = 0\,, \tag{2.26}$$

in both gauge choices.

2.2.3 Codimension

The fundamental difference between studying bulk plasmons and 2D plasmons, is that for the latter, the charges are confined to to a sheet of one less dimension. The mathematical term for this system is that it's a codimension 1 system. It can be shown that for plasmons, the codimension is a very important quantity, more so than the number of dimensions of the system itself. One straightforward way to show this is to compute the contributions to the Coulomb potential[1] of a system,

$$\delta\phi(t, \boldsymbol{r}) \;=\; \int \mathrm{d}^3 r' \frac{\delta\rho(t, \boldsymbol{r}')}{4\pi|\boldsymbol{r} - \boldsymbol{r}'|}\,. \tag{2.27}$$

[1] The concerned reader may worry about the instantaneous-looking Coulomb potential, but will find that it indeed still preserves causality, see e.g. [17].

Keeping the system homogeneous in all three dimensions, returns the previous result of (2.25). However, confining the charges to a plane by factoring in a delta function in one direction yields a different result,

$$k^2\phi - \frac{|k|}{2}\rho = 0\,, \tag{2.28}$$

in Coulomb gauge, and after switching to $\phi = 0$ gauge,

$$\omega^2 A_x + \frac{|k|}{2}J_x = 0\,. \tag{2.29}$$

2.3 Dispersion relations

Equations such as (2.19) are generic for any Maxwell theory, but say very little about the response of any given material. To make a prediction, one needs to further model the compound in some fashion. Where this thesis aims to target strongly coupled materials for which no standard condensed matter theory models are properly available, it is instructive to first consider weakly coupled matter and the already existing models for such.

2.3.1 The Drude model

The most famous one is probably the Drude model of electrical conduction, which considers collisions of electrons moving in a positively charged lattice with a mean free time of τ, without accounting for any long-range interaction between electrons and lattice or other electrons.

The dynamics are described as

$$\langle \mathbf{p}(t+dt)\rangle = \left(1 - \frac{dt}{\tau}\right)\left(\langle \mathbf{p}\rangle + \mathbf{F}dt\right)\,, \tag{2.30}$$

that is, the time evolution of the momentum is given by the fraction that does not collide times their aggregated momentum due to some force $\mathbf{F}$. To first order in dt, this simplifies to

$$\frac{\partial \mathbf{p}}{\partial t} = -\frac{\mathbf{p}}{\tau} + \mathbf{F}\,. \tag{2.31}$$

In our case, we can relate the momentum to the current by

$$\mathbf{j} = -\frac{ne}{m}\mathbf{p}\,, \tag{2.32}$$

where e and m are the charge and mass of the electron, and n is the number density.

For an AC electric field, the force is given by

$$\mathbf{F} = -e\mathbf{E}(t) = -e\mathbf{E}\,e^{-i\omega t}\,, \tag{2.33}$$

and the momentum can be assumed to take the same form, $\mathbf{p}(t) = \mathbf{p}\, e^{-i\omega t}$, which yields a conductivity

$$\sigma(\omega, \boldsymbol{k}) = \frac{ne^2}{m} \frac{\tau}{1 - i\omega\tau} \,. \tag{2.34}$$

This, inserted in (2.16) and (2.19), yields

$$\omega = \frac{-i \pm \sqrt{-1 + 4\tau^2\omega_p^2}}{2\tau} = \pm\,\omega_p - \frac{i}{2\tau} + \mathcal{O}(\tau^{-2}) \,, \tag{2.35}$$

where we have defined the plasma frequency,

$$\omega_p = \sqrt{\frac{ne^2}{m\epsilon_0}} \,. \tag{2.36}$$

For a propagating wave, $\mathbf{E}(t, \boldsymbol{x}) = \mathbf{E}\, e^{-i\omega t + i\boldsymbol{k}\cdot\boldsymbol{x}}$, the momentum will once again mirror the form, $\mathbf{p}(t, \boldsymbol{x}) = \mathbf{p}\, e^{-i\omega t + i\boldsymbol{k}\cdot\boldsymbol{x}}$, but as the current picks up a spatial dependence, so does the number density, significantly complicating the derivation. This means that there will locally be density variations, which in turn gives pressure variations that will affect the dynamics as well.

2.3.2 Navier-Stokes

One way of modelling the behaviour of a propagating wave is using linearized Navier-Stokes equations,

$$\frac{\partial \mathbf{j}(\mathbf{r}, t)}{\partial t} = -\frac{\mathbf{j}}{\tau} + \frac{n_0 e^2}{m} \mathbf{E}(\mathbf{r}, t) - \beta^2 e \nabla \delta n(\mathbf{r}, t) \,, \tag{2.37}$$

where β is a temperature dependent coefficient. For an ideal gas,

$$\beta^2 = \frac{\gamma k_B T}{m}. \tag{2.38}$$

Using the continuity equation

$$e\frac{\partial \delta n}{\partial t} + \nabla \cdot \mathbf{j} = 0 \,, \tag{2.39}$$

and considering individual frequencies and wavenumbers (ω and k) by imposing $\mathbf{E}(t, \boldsymbol{x}) = \mathbf{E}\, e^{-i\omega t + i\boldsymbol{k}\cdot\boldsymbol{x}}$, and $\mathbf{j}(t, \boldsymbol{x}) = \mathbf{j}\, e^{-i\omega t + i\boldsymbol{k}\cdot\boldsymbol{x}}$ one arrives at

$$\sigma = \frac{n_0 e^2}{m} \frac{i\omega}{\omega^2 - \beta^2 k^2 + i\omega/\tau} \,. \tag{2.40}$$

Inserting this conductivity in (2.16) and (2.19) gives the dispersion relation

$$\omega = \pm\sqrt{\omega_p^2 + \beta^2 k^2} - \frac{i}{2\tau} + \mathcal{O}(\tau^{-2}) \,, \tag{2.41}$$

with ω_p defined as in (2.36). An important thing to note here is that the scale β introduced by the Navier-Stokes equation is not directly dependent on τ, but are in simpler systems (e.g. an ideal gas or fluid) proportional to the temperature T.

Similarly, inserting (2.40) into (2.29) yields

$$\omega = \pm\sqrt{\left(\beta^2 k + \omega_p^2/2\right)}\sqrt{k} - \frac{i}{2\tau} + \mathcal{O}(\tau^{-2})\,, \tag{2.42}$$

which is interesting for two particular reasons. First of all, for small k (and large τ), it goes as

$$\omega \propto \sqrt{k}\,, \tag{2.43}$$

which is a famous result for 2D materials. Furthermore, the damping term becomes increasingly important for small k. An expansion in small k, and generic τ, instead reveals two purely imaginary, i.e. non-propagating modes

$$\begin{cases} \omega = -\dfrac{1}{2} i\tau\omega_p^2 k + \mathcal{O}(k^2)\,, \\ \omega = -\dfrac{i}{\tau} + \dfrac{1}{2} i\tau\omega_p^2 k + \mathcal{O}(k^2)\,. \end{cases} \tag{2.44}$$

2.3.3 Other models

Plasmon dispersions can be studied theoretically in various different ways in different number of dimensions, see e.g. [18] for some other weakly interacting examples, both treated classically and with QFT methods. As mentioned above, it is not necessarily that the charges are free to move in a three-dimensional bulk, or that they are confined to a two-dimensional plane that is of importance for the characteristics of the modes above, but that they are confined to move in the same number of, respectively one less, dimensions than the electromagnetic fields. This means that we would expect essentially the same behaviour if the total number of spatial directions were two, rather than the three we experience daily. This may not seem important for a non-theoretician, but in the language of the AdS/CFT-correspondence we introduce later, it is.

It is also worth mentioning that due to the close relationship between the dielectric function and the conductivity (2.16), observations of the latter can be used to find dispersion relations for collective modes. It is thus a simple matter to verify that the conductivity found in e.g. [19] also yields the characteristic $\omega \propto \sqrt{k}$ dispersion, even though that particular computation is carried out for the Dirac fluid phase of graphene, which is strongly coupled - i.e. the arguments in the previous section does not hold.

The same relation has also been found in other studies with conventional condensed matter techniques such as the random phase approximation (RPA) and self-consistent field approximations [20, 21].

The 2D plasmon dispersion has also been experimentally observed in graphene, see e.g. [22–24].

While the 3D bulk plasmon for metals is well studied experimentally, it has only recently been partly available to observe experimentally in strange metals with momentum-resolved electron energy-loss spectroscopy [25, 26].

Chapter 3

Strange metals

In this chapter we will discuss some of the problems arising due to strong coupling in certain materials, often called strange metals.

In the previous chapter we treated electrodynamical response in some classical models. With a weak electromagnetic coupling strength, these model works well (for the purpose of this thesis at least). Quantum mechanically, the coupling strength has many interpretations, but the most clear one is a proportionality to how likely a charged particle is to emit or absorb a photon. This can in turn be expressed in terms of Feynman diagrams, where such an interaction is of the form of a particle going in to the interaction point, and a particle and a photon going away. The likelihood of each such vertex is related to the bare coupling strength, meaning that for a small interaction strength, diagrams with more vertices are less likely, and may at some point be negligible. For small coupling strength, it is therefore relevant to consider expansions in the coupling parameter, where to get some arbitrary precision, you can include all possible diagrams with up to n vertices, as essentially other diagrams are suppressed by order α^n, which is very small, and thus gives rise to a very small error. This is the foundation of perturbation theory, which is one of the most successful tools used in condensed matter theory. In a vacuum, the electromagnetic coupling strength is about $1/137$, which is definitely small enough for perturbation theory to provide an accurate description.

However, in many theories one is not that fortunate. Remarkably, this is not a problem as often as one would initially expect. For instance in most metals, the coupling strength is about order one, which would imply that the higher order terms would not be negligible to any expansion order. Due to a very fortunate circumstance, they are often able to be described with Fermi-Landau theory as Fermi-liquids. Liquid here being a keyword implying that they are strongly coupled, but practically still a continuation of the weakly coupled electron gas. This holds essentially because the theory works at small coupling strengths, and while continuously turning up the

coupling constant from small values, the theory passes no poles, no phase transition occurs and one would thus expect a similar behaviour [27].

However, as stated above, this is not what one would have expected but rather a common, and fortunate, special case. Metals could just as well have had a phase transition, which would leave us in the dark about how the next phase worked. What we do know about this new phase is that it is found were one would ordinarily expect a metallic phase, but the excitations are not well described by the electron-hole pair quasi-particles of Fermi-Landau theory. And from this follows the fitting name of "strange metals".

Although quantum field theory struggles to describe these phases, there has been some success with the random phase approximation (RPA) method. In this method, one argues that, largely from symmetries, that many of the contributions from the diagrams can be neglected due to cancellations. Instead a specific sequence of diagrams are summed, which can analytically be summed, specifically the sequence presented in figure 3.1.

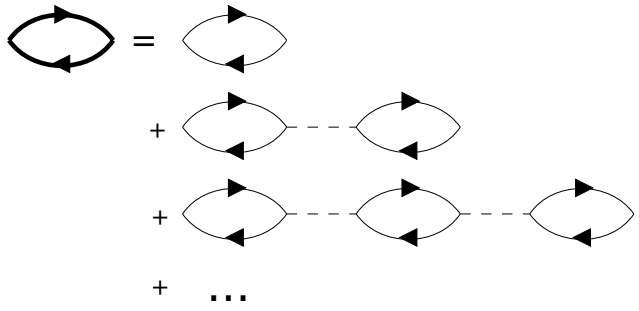

Figure 3.1: Feynmann diagrams summed in the RPA. On the left side, in bold, is the full Green's function, and on the right side the non-interacting Green's function as lines and the interaction photon dashed.

In terms of the interaction potential V, and the screened correlator χ_{sc}, the full correlator χ is given as

$$\begin{aligned}\chi(\omega, \boldsymbol{k}) &= \chi_{sc} + \chi_{sc} V \chi_{sc} + \chi_{sc} V \chi_{sc} V \chi_{sc} + \dots \\ &= \frac{\chi_{sc}(\omega, \boldsymbol{k})}{1 - V(\omega, \boldsymbol{k})\chi_{sc}(\omega, \boldsymbol{k})} \,. \end{aligned} \tag{3.1}$$

This expression is in fact closely related to the similar relation in (2.21), as the denominator in (3.1) becomes the dielectric function via (2.20) and (2.16). Although RPA is primarily used for weak coupling, where the convergence can be argued, it has also had some success for strongly coupled systems, where the motivation behind the approximation somewhat falls short.

However, where the usefulness of conventional condensed matter methods is limited, holography steps up as an exceptional candidate to provide

theoretical descriptions and predictions of such phases. This has been an endeavor for some time now [28] and has been remarkably successful [29, 30].

There are primarily two different types of strange metals observed, and they are in some ways related. High temperature superconductors display that behaviour at temperatures above the superconducting phase, and graphene (and possibly other newly discovered 2D materials) when doped to near charge neutrality [31]. As the high temperature superconductors are layered materials, they are dimensionally related, even though one of them is a bulk material (i.e. 3D) and the other a sheet.

3.1 High temperature superconductors

High temperature superconductors are materials that become superconducting at temperatures below some critical temperature T_c, that is large compared to what could be expected from BCS-theory, about 30 K. Where there is still no comprehensive theoretical understanding of this phase, there exist partial descriptions, such as resonating valence bond theory. One important observation is however that the mechanism is not an electron-phonon interaction as in BCS-theory, but rather some electronic coupling which varies between different materials.

After the discovery of the first high temperature superconductor, almost all high temperature superconductors for twenty years were variations of that one, layered materials of metallic elements and copper oxides, referred to as cuprates. Today there are also iron based superconductors as the second large group of superconductors, and a few oddballs, such as hydrogen sulfide under extreme pressure.

At temperatures above T_c, cuprates are in the strange metal phase, which is even less well understood than the superconducting phase. This phase displays several intriguing properties, such as Planckian dissipation, T-linear resistivity and a conjectured minimal viscosity [32, 33]. This phase is characterized by strong coupling, possible long-range entanglement and cannot be described by quasiparticles. This essentially cripples conventional condensed matter tools such as perturbation theory and Monte-Carlo methods, but paves the way for a holographic treatment.

3.2 Graphene near charge neutrality

Graphene is as close to perfectly two-dimensional a material can get. A single atom thick, it is a sheet of carbon atoms, arranged in a hexagonal, honeycomb structure. This has some very important ramifications for its properties. Graphene is, despite being thin, incredibly strong and durable. It also has some very interesting electrical properties; it conducts incredibly well, but can be doped to display even further exotic behaviours. There

appears to be innumerable reasons to study graphene, and it turns out strong coupling is one of them.

Although it was in the 21st century graphene was discovered and received attention, it is actually an old theoretical construction, with a model treatment as early as 1947 by Wallace [34]. As graphite is well-known to be composed of multiple weakly connected layers of carbon, a single sheet is a rather natural construction and exactly what graphene is.

Although a theoretical description was available, it took 84 years before Novoselov and Geim produced it and verified that they had indeed found graphene. They were subsequently rewarded with a Nobel prize for their discovery in 2010, and an immense amount of research has since gone into the newly born field of graphene physics. For instance, the European Union started their flagship, investing €1 billion into the vision of graphene being available to consumers by 2025, with Chalmers University of Technology as its base.

As many materials with extreme and exotic properties, graphene has some very interesting potential applications. Because it is thin, miniaturization of circuits. Because it is flexible, bendable electronics. Because it is strong, as discrete reinforcement, and many more.

For the purpose of this thesis, graphene is especially interesting for two reasons. Firstly, there is the Dirac point. At a specific level of doping, the Fermi surface of graphene degenerates to a point, and all electrons are instead bound to their respective nuclei. This results in an effectively neutral system. Near this point, graphene has shown indications of strong coupling, making holography an excellent framework to treat the system [31, 35].

Secondly, the 2-dimensional nature of graphene has some very interesting implications and is the underlying foundation to its other properties. It is therefore important to study strange metals in both two as well as three dimensions.

Chapter 4

Holography

Holography is one of those things in physics that for the uninitiated may seem like witchcraft, and possibly even to those in the field.

The underlying principle is that of a duality, between a QFT and a gravity theory in a larger space. The key interest lies in that one of them can be strongly coupled (usually chosen to be the QFT) while the other is weakly coupled. Then, on the QFT side, we have a theory that is remarkably complex, and practically impossible to treat mathematically, even with the most powerful computers. On the other side, we have something seemingly unrelated and comparatively simple that we have little trouble making calculations and predictions for. The duality makes the bold claim, that they can both be governed by the same dynamics, and the results from one side, can be translated to the other.

The duality has since it's inception grown to encompass a lot more than it's original formulation, and has with increasing generalization and different target applications earned many different names. Most of these are still in use - from the very specific "AdS/CFT-correspondence" as the gravity side should asymptotically be a negatively curved anti-de Sitter (AdS) space, and the other side a conformal field theory (CFT) - to the less specific "gauge/gravity duality" simply denoting what type of theory is on each side - to the very broad name of "holography" indicating a more hands on approach where we project one theory into a larger space, precisely like a hologram. This increasing generality also means less constraints on the QFT, making the duality more enticing for condensed matter theory.

In recent years, several excellent books on the subject have been written for the reader that wants to get into the subject [36–38].

4.1 History

Symmetries have throughout mankind's history always had an almost mythical presence. In art, many forms strive for symmetry, and others strive to

break symmetries for dramatic effects. In society, we see symmetries as a naturally just system, worthy of pursuit. Similarly, symmetries play an intuitive and crucial role in physics. The force exerted by one object onto another is returned with identical size but opposite direction. Gravitational and electromagnetic forces only depend on the distance to an object, resulting in spherical symmetries. Also less obvious, but fundamental symmetries of time and space, if you conduct an experiment (under similar circumstances) it does not matter when or where you conduct the experiment, the very cornerstone of science itself.

The pursuit of symmetries in physics can seem almost maniacal, but as records show, has been correspondingly successful. Both in that there is an intricate relationship between conserved quantities and symmetries (Noether's theorem) – conserved energy corresponds to a time symmetry, conserved momentum to translational symmetry, and many more. Even the fundamental forces of nature corresponds to different symmetries. A lot of theoretical physics is based around understanding symmetries, and the effects of spontaneously or explicitly breaking these symmetries, and has been the driving force behind theories such as supersymmetry, which very naturally occurs in string theory, but not apparently at our energy scale in daily life.

As different physical theories are fundamentally described by their symmetries, different theories with the same symmetries behave very similarly, regardless of how these symmetries arose. This leads to the notion of dualities, where simply describing one system is enough, and where you can translate the results from that system to others that have the same symmetries. Especially in string theory these are prevalent, as the underlying framework has a lot of symmetries (literally supersymmetric), and you can achieve different symmetries by simply breaking some symmetries rather than having to introduce new ones.

There are many important and famous dualities in string theory, but none more so than the AdS/CFT-correspondence, discovered by Maldacena in 1997 [39]. Maldacena noted that the symmetries of the boundary of an anti-de Sitter space in a weakly coupled string theory, mirror the symmetries of a strongly coupled conformal field theory, in particular an SU(N) super Yang-Mills theory for large N, similar to what dominates the rather poorly understood quark-gluon plasma of quantum chromodynamics (QCD), where $N = 3$.

The discovery was remarkable in it's own merit, but it wasn't until the incredible, verifiable predictions of the strongly coupled quark-gluon plasma [40] that the discovery got real attention from non-theorists. Another significant increase of interest came with qualitatve agreements from weakly coupled AdS-spaces to strongly coupled condensed matter field theory (AdS/CMT, that is dualizing with an electromagnetic theory). Not only does there exist applications in condensed matter physics, but there is also

a need for some way to describe strange metals with huge potential benefits of understanding and predicting their behaviours.

The original duality was formulated between a type IIB string theory on $AdS_5 \times S^5$ and a conformal field theory on the boundary of the AdS_5. Stacking N D3-branes in the 10-dimensional spacetime of the string theory results in the mentioned gauge theory in the low energy limit. In this limit, the gauge theory on the D3-branes also decouples from from gravity, and higher derivative corrections to the action are suppressed. The stacked branes constitutes a black hole, with a metric that doesn't quite line up with what is desired. Near the horizon however, the leading order behaviour of the warp factor does give the correct geometry. This consititutes a second limit which provides a more reliable gravity solution, which can be mathematically formulated as $r \ll L$, i.e. the AdS radius of curvature L should be large. This radius directly stems from the influence of the D3-branes, and can be shown to depend on N as

$$L^4 = 4\pi\, N\, l_P^4\,, \tag{4.1}$$

that is, the number of branes (and thus colours in the gauge theory) should be large. This also directly corresponds to the AdS length scale being much larger than the Planck length scale l_P, meaning that quantum gravity effects become small. Similarly, one finds on the gauge theory side of the duality that the effective coupling strength, the 't Hooft parameter λ, has to be large for much the same reasons. This in turn corresponds to the AdS length scale being much larger than the string length l_S, as

$$L^4 = \lambda\, l_S^4\,, \tag{4.2}$$

suppressing the effects of highly excited strings.

Now, the discussion for validity and reliability of the duality is one of great interest and importance. Whereas these limits may seem very restrictive, and justifiably stirs up scepticism to using the duality as a tool, it is not a discussion this thesis will spend any significant time on.

It is worth mentioning that real occurrences, such as that the information of a 3D object passing through the 2D horizon of a real black hole must be preserved on the surface to not violate the unitarity of quantum physics, also implies the existence of a holographic duality without such limitations. Lastly, the duality can also be derived within ordinary gravity theories by directly studying their symmetries and conserved charges [41]. In those situations, there are however no guarantees that the theory is quantum consistent, which is a property that dualities derived from string theory naturally inherits from string theory and is highly relevant for "quantum matter".

4.2 Models

The way Maldacena introduced the duality has become known as a top-down perspective. The idea here is to take everything you want from the field theory (which we will also call the boundary theory) and include it in a string theory setup, building up a complex gravitational theory, that very accurately describes the known boundary theory. Another, different approach is that, since the boundary theory one wishes to describe in the CMT, is not an SU(N) with large N, one might as well take a known bulk theory, and see what it describes on the boundary. These are known as bottom-up models, and they have the benefit that bulks that are simpler can be perturbed in a manner to include various concepts that would otherwise be rather difficult to include in a controlled top-down manner.

One effect that is difficult to include in a top-down model is a dynamical metric. To include such effects, one would need to include how the presence of D-branes would back-react the metric. This significantly complicates the necessary models relative to the commonly used probe brane models where, under the assumption that the number of probe branes is very small, back-reaction can to some extent be neglected (hence the name "probe"). In general, such probe-brane systems have been quite successful, but for the application of collective modes, the dynamical gravity effects of the embedding appears insufficient to emulate real plasmons and collective modes.

Thus, in this thesis, we focus primarily on bottom-up systems.

4.3 Bulk Theory

The strongly coupled QFT and the weakly coupled gravity theory are linked together by a "geometrization" of the renormalization group scale of the QFT. This essentially means that one adds a new "energy dimension" to the QFT, and in that extended spacetime the gravity theory lives. This naturally gives a notion of a *boundary* theory (the QFT) and a *bulk* theory (the gravity theory).

In the other end of the energy dimension, one finds a black hole. This black hole corresponds to the temperature of the boundary theory, where the black hole has a matching Hawking temperature. It should be noted however that the black hole has an infinite extension, unlike black holes astronomers may find. A "real" black hole is in this setting referred to as a spherical black hole, i.e. it located at some point and extends some distance away to what is known as its horizon. A holographic black hole is infinitely extended in all dimensions but the energy one, and extends some (finite) distance also in that one. If the boundary has two spatial directions, the black hole is located on a mathematical plane and is thus called *planar*, as

pictured in figure 4.1. As such, it would arguably be more fitting to refer to them as black planes, or as is done in string theory, black branes. We opt, as is often done, to keep the familiar terms, even in calling the distance to the black hole a radial distance.

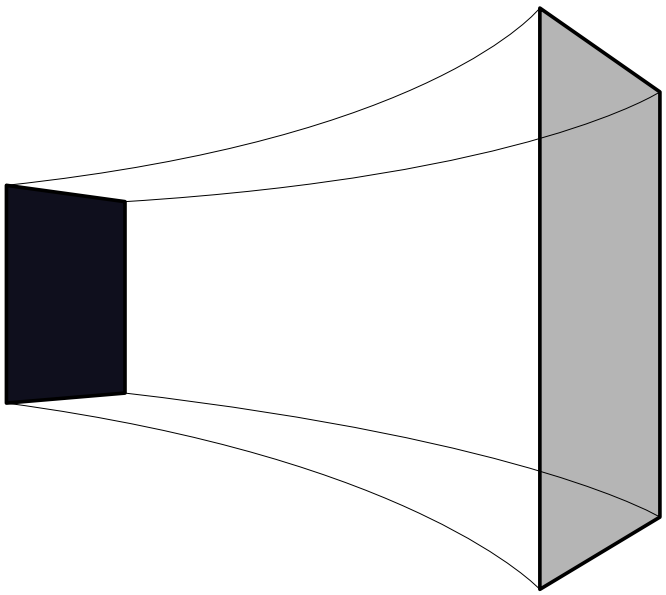

Figure 4.1: The basic holographic setup. To the left, at the "bottom" is the horizon of a (planar) black hole, and the gray surface to the right is referred to as the boundary. The volume in between is referred to as the bulk.

A non-zero chemical potential on the boundary, is similarly reflected in the charge of the black hole, and can be read off as the boundary value of the gauge potential in the bulk. Other quantities of the boundary theory can be similarly translated from the bulk theory, according to what is commonly referred to as the holographic *dictionary*.

The essence of this dictionary is formally captured in the famous Gubser-Klebanov-Polyakov-Witten (GKPW) formula, which equates the generating functional of the boundary theory to the partition function of the bulk theory,

$$Z_{QFT}[\{h_i(x)\}] = Z_{Gravity}[\{h_i(x)\}]. \tag{4.3}$$

That is, the generating function of an operator $\mathcal{O}_i$ with source h_i in the boundary theory,

$$Z_{QFT}[\{h_i(x)\}] \equiv \left\langle e^{i\sum_i \int dx h_i(x)\mathcal{O}_i(x)} \right\rangle , \tag{4.4}$$

matches the partition function of the bulk theory with a bulk field ϕ_i, cor-

responding to $\mathcal{O}_i$, which takes the boundary value h_i

$$Z_{Gravity}[\{h_i(x)\}] \equiv \int^{\phi_i \to h_i} \left(\prod_i \mathcal{D}\phi_i \right) e^{iS[\{\phi_i\}]} \,. \tag{4.5}$$

This is visually represented in figure 4.2.

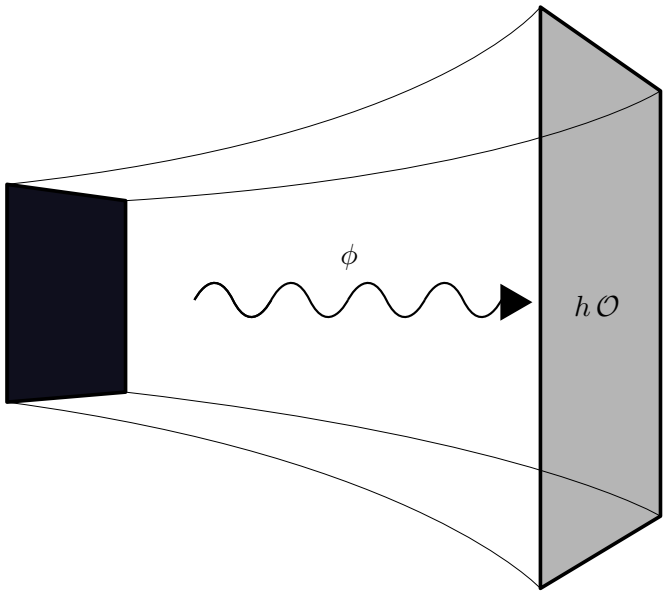

Figure 4.2: The holographic dictionary: A bulk field ϕ's boundary value h, is the source of a QFT operator $\mathcal{O}$. As an example, a bulk electric flux from a charged black hole yields a charge density in the boundary theory.

The temperature and chemical potential are in many ways the fundamental building blocks for a holographic description. In the bulk, they are linked together via the Einstein-Maxwell action with a cosmological constant, Λ, that ensures the asymptotic AdS geometry. This yields the familiar Lagrangian

$$\mathcal{L}_{ME} = -\tfrac{1}{4} F_{\mu\nu} F^{\mu\nu} + \tfrac{1}{2}(-2\Lambda + R), \tag{4.6}$$

where R is the Ricci scalar found in general relativity and we have chosen to work in natural units[1].

Varying the action (4.6) with respect to the metric g and the gauge potential A yields a set of equations of motion which can be solved to find the values of the respective fields at any given point and time. These are

[1] That is, units chosen such that most physical constants, such as the speed of light, are one.

obtained as

$$0 = -\nabla_\kappa \nabla^\kappa A^\mu + \nabla_\kappa \nabla^\mu A^\kappa \,, \tag{4.7}$$

$$0 = -\Lambda g^{\mu\nu} - \tfrac{1}{4} g^{\mu\nu} F_{\kappa\lambda} F^{\kappa\lambda} + F^{\mu\kappa} F^{\nu}{}_{\kappa} - R^{\mu\nu} + \tfrac{1}{2} g^{\mu\nu} R \,. \tag{4.8}$$

4.3.1 Background solution

As it is by far the most convenient to work in linear response, we first need to solve for a background and secondly solve for a small perturbation around that background.

While it is also possible to study systems at zero temperature, we opted to study cases with non-zero temperature, which are experimentally most relevant. This allows us to define our coordinate system with the "radial/energy" coordinate z such that the black hole's event horizon is located at $z = 1$ and the boundary is located at $z = 0$. This effectively means redefining the coordinates as $z = r_H/r$ in the more conventional coordinate system where $r = r_H$ is the location of the black hole horizon and the boundary is located at $r \to \infty$.

We assume the background to be static (unchanging in time), and in the spatial directions, homogeneous and isotropic (unchanging with position and similar in all directions). In a $(3+1)$-dimensional bulk we can make an ansatz for the metric as

$$L^{-2}\,\mathrm{d}s^2 = L^{-2} g_{\mu\nu}\,\mathrm{d}x^\mu x^\nu = -f(z)\,\mathrm{d}t^2 + z^{-2}\,\mathrm{d}x^2 + z^{-2}\,\mathrm{d}y^2 + g(z)\,\mathrm{d}z^2, \tag{4.9}$$

where f and g are functions of the radial coordinate z, and L is the AdS length scale,

$$\Lambda = -\frac{3}{L^2} \,. \tag{4.10}$$

Motivated by isotropy, we can also make an ansatz for the Maxwell gauge field A to only point in the time-direction, i.e.

$$A_\mu = L \begin{pmatrix} h(z) & 0 & 0 & 0 \end{pmatrix} . \tag{4.11}$$

Inserting these assumptions into (4.7) and (4.8) yields three scalar equations of motion,

$$0 = 4fg + gzf' + fzg' \,, \tag{4.12}$$

$$0 = -2f + 6fgz^2 + 2zf' - z^2\big(h'\big)^2 \,, \tag{4.13}$$

$$0 = h'' \,, \tag{4.14}$$

where prime denotes a radial derivative. These are solved by

$$f(z) = \frac{c^2}{z^2} - Mz + \frac{1}{2} Q^2 z^2 \,, \tag{4.15}$$

$$g(z) = \frac{c^2}{z^4 f(z)} \,, \tag{4.16}$$

$$h(z) = \mu - Qz \,, \tag{4.17}$$

meaning that the background has four free parameters, c, M, Q and μ. The chemical potential μ is fixed by requiring the Maxwell potential to disappear on the horizon,

$$h(1) = 0 \Rightarrow \mu = Q, \tag{4.18}$$

which would otherwise cause a gauge singularity. As we have rescaled the radial coordinate to have the horizon at $z = 1$, this in turn sets a restriction on the mass,

$$f(1) = 0 \Rightarrow M = c^2 + \frac{1}{2}Q^2. \tag{4.19}$$

The speed of light is set by our choice of units,

$$c = 1. \tag{4.20}$$

This leads to a single parameter Q corresponding to the charge of the black hole, that defines the background.

This is the simplest possible bulk model to study holographically. The solution is a planar charged black hole – a Reissner-Nordström (RN) black hole. The boundary theory is referred to as an RN-metal, which should be noted is only a well defined theoretical form of matter, but it should be a fairly good qualitative description of many strongly coupled electron gasses.

It is worth mentioning here that we have chosen the bulk theory to be $(3 + 1)$-dimensional, which means the boundary will only have two spatial coordinates (with time being the "+1"). This may seem more natural for studying surface modes than modes in a bulk, where the charges would normally be free to move in three spatial directions. This is done primarily to simplify things, as in one additional dimension, the Maxwell field exhibits a logarithmic divergence at the boundary. This can be carefully regularized, but those extra steps are not expected to yield significantly different results. Thus it is common to avoid them by studying a (2+1)-dimensional boundary theory, which is what we have chosen to do here.

4.3.2 Perturbation solution

Having solved the relatively simple background, we now turn to a perturbation of this background. The purpose of this is to analyze the dynamics in linear response. The dynamics are otherwise rather difficult and computationally expensive to compute in their full non-linear glory. Working in linear response however, we assume that the changes are small relative to the background. This means that if the perturbations are of order ε, then we can neglect any terms of order ε^2 and higher, since they would then be very small.

This also allows us to Fourier transform our eventual solution meaning we can analyze individual wavelengths and frequencies from the start. Without loss of generality, we assume the wave to travel in the x-direction, which

implies that the time and spatial dependence (on non-radial coordinates) will be $\propto e^{-i\omega t+ikx}$, where we have introduced ω as the angular frequency and k as the wavenumber.

Since the theory is invariant under diffeomorphisms, we can choose to work in radial gauge, i.e. the components $\delta g_{\mu z}$, $(\mu = t, x, y, z)$ and δA_z can be set to zero. Also, as the background is invariant under parity, $y \to -y$, we can chose to study the longitudinal (δg_{tt}, δg_{tx}, δg_{xx}, δg_{yy}, δA_t, δA_x) and transversal (δg_{ty}, δg_{xy}, δA_y) response separately.

Put together, this means we perturb with

$$\delta g_{\mu\nu} = \varepsilon L^2 e^{-i\omega+kx} \begin{pmatrix} \delta g_{\mathrm{tt}}(z) & \delta g_{\mathrm{tx}}(z) & \delta g_{\mathrm{ty}}(z) & 0 \\ \delta g_{\mathrm{tx}}(z) & \delta g_{\mathrm{xx}}(z) & \delta g_{\mathrm{xy}}(z) & 0 \\ \delta g_{\mathrm{ty}}(z) & \delta g_{\mathrm{xy}}(z) & \delta g_{\mathrm{yy}}(z) & 0 \\ 0 & 0 & 0 & 0 \end{pmatrix} \tag{4.21}$$

and

$$\delta A_\mu = \varepsilon L e^{-i\omega+kx} \begin{pmatrix} \delta A_t(z) & \delta A_x(z) & A_y(z) & 0 \end{pmatrix} . \tag{4.22}$$

Perturbing the background solution, i.e. $g_{\mu\nu} \to g_{\mu\nu}+\delta g_{\mu\nu}$ and $A_\mu \to A_\mu+\delta A_\mu$, equations (4.7) and (4.8) become vastly more complex than previously. However, since we are considering linear response we can discard terms of order ε^2 and higher, drastically simplifying the system. Furthermore, order ε^0 is already solved by the background solution.

We are left with a system of nine coupled second order linear ODEs (from the g_{tt}, g_{tx}, g_{ty}, g_{xx}, g_{xy}, g_{yy}, A_t, A_x and A_y components) as well as five constraint equations (from the g_{tz}, g_{xz}, g_{yz}, g_{zz} and A_z components) that serves as a check, as they should hold true if we could actually make the choice of radial gauge we made above. The equations are still rather lengthy, but are included in appendix A for the curious reader.

These equations cannot be solved analytically, and have to be solved numerically[2]. The form of the background provides a specific challenge for a numerical solution as the horizon needs to be addressed. There are multiple ways of dealing with this. From a theoretical standpoint, a coordinate switch to Eddington-Finkelstein coordinates solves the issue, but from a practical standpoint, it is more convenient to factor out an exponential term in the fields and in the equations amounting to a Frobenius expansion.

This is simply done by making an ansatz

$$\begin{aligned} \delta A_t &= (1-z)^{i\alpha} \delta A_t^* , \\ &\dots \end{aligned} \tag{4.23}$$

for the fields, where the star indicates the (regular) field post Frobenius expansion. This ansatz is then inserted into the equations of motion, which

[2]The numerics of the articles this thesis is based on were carried out in Mathematica, and to various degrees utilizing the packages xAct [42] and xTras [43].

are subsequently expanded as a series near the horizon. One finds that two choices of α gives non-trivial solutions, these are frequency dependent, and explicitly one gets near the horizon

$$\delta A_t = (1-z)^{\pm\frac{2i\omega}{6-Q^2}}\delta A_t^* \,. \tag{4.24}$$
$$\dots$$

As the singularity arises from the metric component f, it may be preferable to use $f(z)$ as a base rather than $(1-z)$, which is a common choice for these types of studies. Both the positive and the negative exponent correspond to mathematical solutions, but only the negative one yields *physical* solutions as the exponent can be interpreted as out-going and in-falling solutions, of which only the latter is sensible in regards to a black hole.

In the process of expanding the fields, the singular behaviour of f and g eliminates multiple degrees of freedom. Nine coupled second order ODE's are expected to be defined up to initial values of each field and their first derivative, i.e. 18 degrees of freedom, of which one eliminates half by requiring in-falling boundary conditions. Thus, one would still naively expect to have nine degrees of freedom left, but in this case, there are only four (two longitudinal and two transverse) – the others have been eliminated by the singular behaviour at the horizon. The remaining degrees of freedom can be chosen to be $\delta A_x^*(1)$, $\delta g_{xx}^*(1)$, $\delta A_y^*(1)$ and $\delta g_{xy}^*(1)$.

There are in fact five more solutions that are missed in the treatment above. They are pure gauge solutions from the remaining degrees of freedom in our gauge choice, and as such do not need to fulfill the above mentioned requirements. These are solutions of the form

$$\delta g_{\mu\nu} = \nabla_\mu \xi_\nu + \nabla_\nu \xi_\mu \tag{4.25}$$
$$\delta A_\mu = \xi^\nu \nabla_\nu A_\mu + A_\nu \nabla_\mu \xi^\nu \,, \tag{4.26}$$

and

$$\delta A_\mu = \nabla_\mu \zeta \,, \tag{4.27}$$

for some ξ or ζ. A similar treatment is made in [44]. These solutions can be found analytically, but we do not include them here as some are quite long.

Thus, there are nine linearly independent solutions, and any linear combination of these is also a solution to the equations of motion. To get a unique solution, one needs to implement nine additional boundary condition at the conformal boundary.

4.4 Boundary conditions

The boundary conditions to enforce on the conformal boundary are closely related to the boundary theory itself. In a sense, the parameter Q and the

horizon radius r_H that we eliminated from the equations by changing our coordinate system are also determined by the boundary theory. They are both closely related to the temperature and the chemical potential of the boundary theory.

The (Hawking) temperature can be identified by Wick rotating. Near the horizon, the Euclidean time is periodic with the inverse temperature as period, leading to

$$T = \frac{6 - Q^2}{8\pi} \frac{r_H}{L^2} \,. \tag{4.28}$$

The holographic dictionary identifies the boundary field strength $\mathcal{F}$ and the boundary current $\mathcal{J}$,

$$\mathcal{F} \;=\; \frac{1}{\sqrt{\lambda}} F\big|_{\partial M} \,, \quad \mathcal{J} \;=\; \sqrt{\lambda}\, \imath_n W\big|_{\partial M} \,, \tag{4.29}$$

from the bulk field strength F and the bulk induction tensor W (composed by $\boldsymbol{E}, \boldsymbol{B}$ and $\boldsymbol{D}, \boldsymbol{H}$ respectively). Here we have introduced the parameter λ which relates the coupling strength for electromagnetism on the boundary theory with the one in the bulk. They do not necessarily have to be equal (which would correspond to $\lambda = 1$). This ultimately leads to the chemical potential μ being

$$\mu = \frac{Q}{\sqrt{\lambda}} \frac{r_H}{L^2} \,. \tag{4.30}$$

That means, given a specific chemical potential μ and a temperature T on the boundary, there exists values of r_H and Q in a the bulk that yields those values on the boundary. As the horizon radius does not enter into the ODE's we solve, it is convenient to use the dimensionless quantity μ/T on the boundary to describe different boundary theories as it only depends on Q.

This means that (up to rescaling), all RN-metals at the same μ/T behave similarly. Furthermore, the charge density can also be uniquely determined from the holographic dictionary in terms of the chemical potential and the temperature for all such systems,

$$n \;=\; \sqrt{\lambda}\, Q \frac{r_H^2}{L^2} \;=\; \frac{2}{3}\pi\lambda\mu T L^2 + \frac{1}{6}\lambda\mu L^2 \sqrt{6\lambda\mu^2 + 16\pi^2 T^2} \,. \tag{4.31}$$

This constraint does not hold for most boundary theories, so to model more realistic systems one needs to include another scale into the system, something that is done in e.g. the electron cloud model we look at in paper IV.

Similarly, the boundary conditions on the perturbations can be found from properties of the boundary theory. Most notably, since there is no dynamical gravity in the boundary theory (gravitational effects are generally negligible in relevant QFTs), the perturbations of the metric components should vanish on the boundary.

Similar to how the background field A_μ gives rise to a potential and a charge density, the perturbations gives rise to fluctuations in these. In the study of quasinormal modes, the condition (2.26) corresponds to

$$\delta A_t\Big|_{\partial M} = 0\,, \qquad \delta A_x\Big|_{\partial M} = 0\,, \qquad \delta A_y\Big|_{\partial M} = 0\,, \tag{4.32}$$

and these have been studied before, in e.g. [45, 46], and are common to study in almost any holographic system. Even earlier, in the context of "real", spherical black holes, QNMs were studied in [47, 48].

Once a complete set of boundary conditions has been chosen, one can start looking for solutions to the full boundary value problem. It is worth noting that as the equations of motion are linear and homogeneous, and the boundary conditions themselves are also homogeneous, the trivial solution (i.e. all fields are zero) is always a possibility. This solution is of course not the desired one, but it does convey an important message – there does not exist a non-trivial solution to the boundary value problem for any ω and k. In fact, what is actually sought after is for what values of ω and k there do exist non-trivial solutions. There exists a non-trivial solution if the nine boundary values of the nine linearly independent solutions are not linearly independent. This is most conveniently examined by evaluating the determinant of the corresponding 9×9-matrix – if they are linearly dependent, it is zero,

$$\left|\begin{array}{ccccccccc} (\delta g_{tt})_1 & (\delta g_{tx})_1 & (\delta g_{ty})_1 & (\delta g_{xx})_1 & (\delta g_{xy})_1 & (\delta g_{yy})_1 & (\delta A_t)_1 & (\delta A_x)_1 & (\delta A_y)_1 \\ (\delta g_{tt})_2 & (\delta g_{tx})_2 & (\delta g_{ty})_2 & (\delta g_{xx})_2 & (\delta g_{xy})_2 & (\delta g_{yy})_2 & (\delta A_t)_2 & (\delta A_x)_2 & (\delta A_y)_2 \\ (\delta g_{tt})_3 & (\delta g_{tx})_3 & (\delta g_{ty})_3 & (\delta g_{xx})_3 & (\delta g_{xy})_3 & (\delta g_{yy})_3 & (\delta A_t)_3 & (\delta A_x)_3 & (\delta A_y)_3 \\ & & & & \cdots & & & & \end{array}\right|_{z\to 0} = 0\,. \tag{4.33}$$

As the calculations are done numerically, one needs to specify some sufficiently strong precision.

Procedurally, this is rather straight forward:

- Choose a background, i.e. μ/T.
- Choose a wave number k.
- Guess a (complex-valued) ω.
- Compute the linearly independent solutions to the equations.
- Examine if there is a non-trivial linear combination of these solutions, i.e. compute the determinant.
- Make a better guess of ω, repeat until chosen precision is achieved.

The roles of k and ω can be reversed if desired to - in some context, a complex valued k may be a more common convention.

It is well worth mentioning however, that in these particular (parity-invariant) systems, there is a decoupling of the differential equations into a longitudinal sector (even in y-indices) and a transverse sector (odd in y-indices), with 6 and 3 equations respectively. This considerably speeds up any numerical calculation by considering the 6×6 and 3×3 system separately, rather than the full 9×9 system. Another point to note is that in the neutral system $Q = 0$, gravitational and electromagnetic effects decouple, meaning that these two sectors splits further into a total of 4 decoupled sectors (longitudinal gravitational, longitudinal electromagnetic, transverse gravitational, transverse electromagnetic), simplifying numerics further.

4.5 Other holographic quantities

It is worth mentioning that several properties of the system are only available when not imposing the full set of boundary conditions. For instance, a computation of the conductivity is a computation of the relation between the electric field and the induced current on the boundary, as in (2.13) . This is generally a matrix equation, but considering longitudinal excitations in the system, it can be reduced to

$$\sigma_{||} = \frac{\mathcal{J}_x}{\mathcal{E}_x} = \frac{\lambda}{i\omega L} \frac{\delta A_x'}{\delta A_x}\bigg|_{z\to 0} \tag{4.34}$$

If, for QNMs, one imposes Dirichlet boundary conditions on the electric field (i.e. zero), such a ratio would be nonsensical. However, imposing the other boundary conditions allows us to find a linear combination of the solutions for any given (ω, k), unless specifically chosen on a QNM, which can be used to compute the conductivity of the boundary system. This also then naturally yields the dielectric function via (2.16), and in this particular sense, the dynamic charge response has previously been studied in [49, 50]. It is also especially useful when comparing to experiments, since in experiments one rarely probes at the exact, complex wavenumber and frequency. Instead, what is typically done is to sweep over a range of values and plot spectral functions. This can thus also be done holographically, although as it is less mathematically interesting it is often omitted. Similarly, computations of the conductivity and dielectric function can be used to verify specific "sum rules" that all materials should satisfy [51].

There are of course many more quantities available to holographic methods as well, but these are the ones most relevant to this thesis. Other quantities include e.g. entropy and viscosity, between which one of the most famous

results from holography holds,

$$\frac{\eta}{s} \geq \frac{1}{4\pi}\,, \tag{4.35}$$

the KSS-bound [52].

4.6 Hydrodynamics

Lastly in this chapter, it is pertinent to say a few words on hydrodynamics, as hydrodynamics and holography have been rather successfully linked, since as early as 2002 [53]. This connectedness has evolved into its own version of the duality, the fluid/gravity correspondence [54], and comparisons to hydrodynamics is common in a large portion of the holographic literature.

Hydrodynamics is a framework built on two fundamental properties:

- Conservation laws – certain measurable quantities, such as energy, mass, and charge, are conserved in a system.
- Fluids are assumed to be a continuum – that is, rather than being a system of discrete particles, they are assumed to be continuous.

This last property resonates very well with the strongly coupled notion of no (long-lived) quasiparticles. The assumption is further improved by considering longer time scales and larger distances, that is, at distances much larger than the mean free path and the mean free time of any constituents of a microscopic description. Practically, this translates to considering systems slowly varying over large distances – small wave numbers (k) and small frequencies (ω). It is therefore in this particular limit that holographic and hydrodynamic results are compared. Since we are interested in boundaries with a dynamical Maxwell theory, similar hydrodynamic treatments, such as [55], are of particular use when comparing results.

Chapter 5

Holographic Plasmons

After the summary of well established results in previous chapters, this chapter will put them together in a way that hopefully appears very natural to the reader, as well as highlights the rather natural progress of our research, as laid out by the papers included in this thesis.

5.1 The plasmon condition

The first insight, and cornerstone of the research behind this thesis, is that quasinormal modes, the modes that have generally been studied in holographic models the last two decades, may not be the most interesting modes to study from the perspective of the boundary theory. This statement is therefore also the most controversial, and subsequently comes with some qualifiers.

What is meant with quasinormal modes here are excitations where the field is set to zero on the boundary. One way to circumvent this is essentially by a field redefinition, such that if one field is zero on the boundary, the other satisfies more physically relevant boundary conditions. Adding additional boundary terms is one way to motivate this, and can be cone both in the context of double-trace deformations [56, 57] or anyonization [58]. In fact, this should always be possible if the boundary theory is to make sense as a variational problem.

If there is some additional known information about the boundary theory, in this case that it obeys Maxwell's equations, and this knowledge is not incorporated into the holographic model per default, it may be suitable to include it in the boundary condition.

If we want to study longitudinal plasmons in a strongly coupled medium, we know they will obey Ampère's law,

$$-\epsilon_0 \dot{\boldsymbol{E}} = \boldsymbol{J} \tag{5.1}$$

and from any holographic model we can extract both the electric field

strength $\boldsymbol{E}$ and the current $\boldsymbol{J}$. These quantities can be read off on the boundary of the bulk theory, and thus for any boundary theory where one wishes to uphold Ampère's law, (5.1) translates into a condition on the boundary values of the fields – a boundary condition.

Depending on the bulk model, this boundary condition may look different, primarily due to how the holographic dictionary identifies the boundary current from every bulk field that couples to the boundary gauge potential $\mathcal{A}_\mu$,

$$\mathcal{J}^\mu = \frac{\delta S}{\delta \mathcal{A}_\mu} \,. \tag{5.2}$$

However, from a bulk model with only a Maxwell lagrangian including the gauge potential near the boundary, the current simply becomes proportional to the sub-leading term of the gauge potential, and specifically in the model detailed in chapter 4, the boundary gauge field is given by

$$\mathcal{A}_x = \frac{1}{\sqrt{\lambda}} \delta A_x|_{z\to 0} \,, \tag{5.3}$$

and the boundary current by

$$\mathcal{J}_x = -\sqrt{\lambda}\delta A'_x|_{z\to 0} \,. \tag{5.4}$$

Put into (5.1), the boundary condition becomes

$$\left(\omega^2 \delta A_x + \lambda \delta A'_x\right)\big|_{z\to 0} = 0 \,, \tag{5.5}$$

where once again, we're working in linear response. This equation we refer to as the (longitudinal) plasmon condition, and this boundary condition replaces the Dirichlet boundary condition $\delta A_x|_{\partial M} = 0$. This boundary condition can equivalently be derived as a double-trace deformation of the boundary [59, 60]. With longitudinal plasmons being the most commonly discussed ones, together with the simplest model possible (detailed in the previous chapter), their union form the starting point for holographic studies of plasmons. This starting point describes bulk, or codimension-0, plasmons i.e. plasmons where the electric charges live in the same number of dimensions as the electromagnetic field, in a strange metal. As such, it is the simplest starting point to describe the plasma oscillations of the more typical high-temperature superconductors at temperatures above the critical temperature.

This model was studied over two papers, paper I which serves as a proof of concept, as well as highlighting experimental agreement and the mathematical reliability of the method, and paper III which highlights the discovery of a "strange" behaviour of the strange metal, in parameter regions inaccessible to other methods and, so far, experiments. This behaviour takes the shape of an exotic dispersion in the transition between a system at large chemical potential and systems at very small or zero chemical potential.

Although the AdS_4-Reissner Nordström metal is the simplest possible model to describe a system at a non-zero temperature and non-zero charge density, there is a lot we can learn from studying the RN-model.

In the Schwarzschild case, i.e. $Q = 0$, we find that of the lowest three modes in the spectra of quasinormal modes (QNM) and collective modes (CM), two are identical. These two modes can be identified as the sound modes in either direction[1]. Upon further inspection, this is very natural - at $Q = 0$ the 6 differential equations decouple into two sets, one consists of 4 gravitational equations and the other consists of two electromagnetic equations. Since the QNM and CM spectra only differ in their boundary conditions in the electromagnetic sector, solutions to the first set will thus be modes in both spectra.

Turning up Q, lets us follow how these modes change, and we find that the QNM remains similar, but the CM gets gapped and becomes what is recognized as the plasmon mode. From this we can understand the importance of the dynamic metric. The origin of the strongly coupled plasmon mode lies in the equations of motion for the metric itself, explaining why probe-brane models in top-down holography have failed to describe plasmons. This suggests that any top-down model that aspires to do so have to in some way take into consideration back-reaction of the brane-embeddings, significantly complicating such models.

Furthermore, we find that the plasmon mode has a non-vanishing imaginary part even at infinite wavelengths, meaning that it is strongly damped. This is hardly surprising for a quantum entangled system of collective excitations at a non-zero temperature, and is a result of the strong coupling, compared to where weak and classical results do have stable plasmons at very long wavelengths.

Lastly, we find that the transition between sound at $Q = 0$ and a plasmon at large Q is not a simple one. The most naive way of imagining such a transition would simply be to "lift" the real part of the mode with Q. This is not what happens, and it can be argued for in several ways. One of the more compelling ways is to consider the number of hydrodynamical modes, $\omega(k \to 0) \to 0$, which corresponds to conserved quantities in the theory. By introducing a charge density with Q, we break a symmetry and should thus have one less hydrodynamical mode. A small change in Q should mean a small change in the mode, and thus the change should be located mostly near the origin. The sound mode is technically two modes, with a positive of negative sign of the real part differentiating between directions. Due to the symmetry in both directions, separating the two modes can only be done if this real part becomes zero, and that is essentially all that happens.

For the mode to then become gapped again, that purely imaginary mode

[1]Note that these sound modes are not ordinary sound, i.e. phonons in the lattice, but are phenomenologically similar.

must merge with another, higher, purely imaginary mode, but since we should still keep the hydrodynamic imaginary mode (the diffusive mode), it has to merge with another purely imaginary mode. Once again this is what we see in our model, and although seemingly exotic with several physical implications, there aren't really alternative ways such a transition could take place.

5.2 Codimension-1 models

The next natural step for the research is to target strange metals in the same category as graphene, i.e. codimension-1 materials. In this context, the model described in chapter 4 is arguably even better suited for describing graphene than it is for describing cuprates. This is true for primarily two reasons. Firstly, cuprates are rather "messy" materials, with a lot of internal structure and a layered composition that is not captured in such a simple model. Secondly, the true number of spatial directions for charges is two, in both graphene and the model. That being noted, the number of dimensions for the EM field is also two, and instead of simply applying Ampère's law again, the missing third dimension has to be taken into account already in the boundary condition. This is a rather straightforward integration, and yields the result of equation (2.29),

$$\omega^2 A_x + \frac{|k|}{2} J_x = 0\,, \tag{5.6}$$

and into that equation we can insert the holographic results. This work is carried out in paper II.

Once again, although it is the simplest possible model, and with some corners cut in order to confine charges to a plane while the electromagnetic fields are allowed to propagate in the full space, it is remarkable how well the model performs.

For neutral systems, due to how the boundary conditions are constructed, the sound mode is preserved as it lies in the gravitational sector, just as for bulk systems.

In charged systems, we find the characteristic $\sqrt{k}$-dispersion of 2DEG materials, but as we are once again free to change the charge Q, we can examine more closely how such a transition would look like for small charge densities. Although we find no surprising additional effects, it is noteworthy how well the model captures the results of other methods that are only valid in some extreme limits [61, 62], while smoothly transitioning between them in the intermediary regions where no proper descriptions were available before.

5.3 The electron cloud

The RN bulk model that has been covered up to this point is a rather simple model, and may for some considerations be just a bit too simple.

The fact that we cannot tune temperature, chemical potential and charge density as three independent parameters and effectively only have one parameter is an apparent weakness. To address this, one would need to implement additional scales in the system.

Another important note is that if the bulk theory supports charged particles, the RN black hole is unstable [63–65]. If the temperature of the black hole is decreased (Q is increased), the local chemical potential in the bulk is eventually large enough to support a density of such charged particles, leading to pair production and hence an instability. The extremal solution ($Q = \sqrt{6}$) is then never reached. This is in essence a good thing; the extremal solution has other problems which arise when there is effectively a double event horizon. However, it does mean that the static RN bulk background is not sufficient at low temperatures. This feature is well established and if the particles are charged scalars, the bulk scalar condenses at low temperatures, which is what results in holographic superconductors [66, 67].

If instead the charged particles in the bulk theory are fermions, the bulk may for large enough Q support a density of those at a distance outside of the horizon, as in figure 5.1. We refer to such a setup as an "electron cloud"[68]. It is worth noting that these charged particles are not the same as the electrons on the boundary, but merely a name reflecting their nature. Gradually decreasing the temperature increases the extent of the cloud and ultimately, the bulk collapses into an "electron star" [69], which has several similarities to a neutron star.

That collapse is however of limited interest here for several reasons. Firstly, if the bulk also supports a scalar of greater mass, then that would also contribute at low temperatures. Secondly, for lower temperatures of the black hole, the temperature of the electron cloud becomes increasingly important. From a computational perspective, this is non-trivial as one of the most important simplifications typically done is to assume that the cloud is cold. This makes the inner and outer limit of the cloud seen in figure 5.1 well defined. Instead, having a Fermi-Dirac distribution of the particles in terms of the local chemical potential would mean that for any non-zero temperature of the cloud, the cloud would stretch all the way from the horizon to the conformal boundary. This causes a wide range of difficult issues, including the need for a radiative description of the black holes collapse. Thirdly, by keeping the previous description of the RN hole, we indirectly close the door of such a collapse as we normalize with the horizon radius, which would not be applicable in a system without a black hole.

But as a first step in such a mode of instability, the electron cloud is an interesting model. Furthermore, the mass and charge of such fermions in-

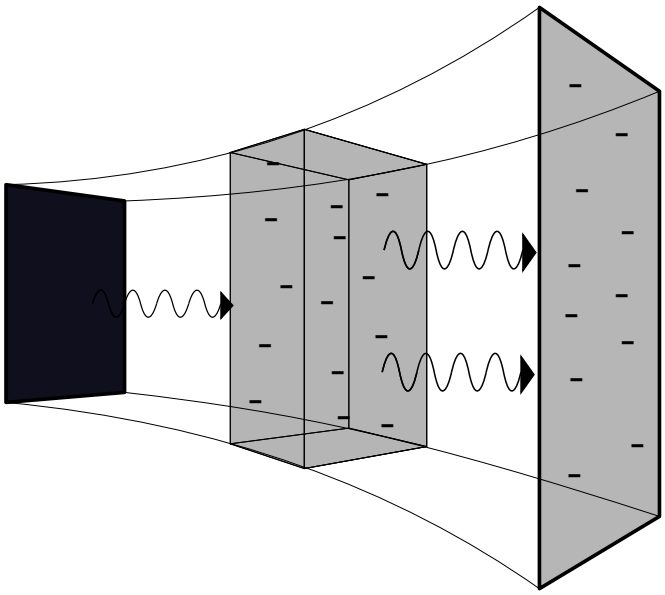

Figure 5.1: The electron cloud bulk. If the mass of the charged fermion and the temperature of the black hole is sufficiently low, there will exist a region between the black hole and the boundary in which a density of fermions are supported.

troduce two additional scales which would allow us to tune the temperature, chemical potential and charge density of the boundary system independently.

The Einstein-Maxwell action (4.6) is for the electron cloud extended with the Lagrangian of a charged, non-rotating, zero temperature, perfect fluid [70],

$$\mathcal{L}_{fl} = -\rho_{\text{fl}}(n) + nu^{\mu}A_{\mu} + nu^{\mu}\partial_{\mu}\phi + \lambda\left(1 + g_{\mu\nu}u^{\mu}u^{\nu}\right) , \tag{5.7}$$

where ρ_{fl} and n are the energy density and number density respectively. The charge of the fluid particles has been set to unity. ϕ is a 'Clebsch' potential that ensures that the mass of the fluid is conserved. Similarly, λ is a Lagrange multiplier implementing that u^{μ}, the local fluid velocity, squares to minus one, as required for the 4-velocity.

The local chemical potential in the bulk is then

$$\mu_{loc} = u^{\mu}\left(A_{\mu} + \partial_{\mu}\phi\right) . \tag{5.8}$$

It should be mentioned that this local chemical potential in the bulk can also be used outside the electron cloud, as it is the factor n that makes the contribution to the Lagrangian vanish, meaning that it is a well defined quantity even for the pure RN solution (the contribution from the 'Clebsch' potential will however vanish). The cloud is supported when the local bulk chemical potential is larger than the mass of the fermions, m.

Approximated in the Thomas–Fermi limit, the density of states is

$$D(E) \;=\; \beta E\sqrt{(E^2-m^2)}\,, \tag{5.9}$$

for energies above the cloud particle mass m, and where β is a parameter determining the density of the cloud, not to be confused with the β in chapter 2. This sets the number density and the energy density inside the cloud as

$$n \;=\; \int_m^{\mu_{loc}} D(E)\,\mathrm{d}E\,, \qquad \rho_{fl} \;=\; \int_m^{\mu_{loc}} E\,D(E)\,\mathrm{d}E\,, \tag{5.10}$$

respectively. The pressure is then given by the usual equation of state,

$$p \;=\; -\rho_{fl} + n\mu_{loc}\,. \tag{5.11}$$

Variations with respect to the introduced fields in most cases correspond to algebraic constraints, which can directly be used to eliminate fields from the equations of motions which need to be solved. The background solution for u is

$$u^\mu = L^2\left(\;\sqrt{f(z)},\quad 0,\quad 0,\quad 0\;\right), \tag{5.12}$$

with the longitudinal perturbation

$$\delta u^\mu = \varepsilon L^2 e^{-i\omega t+ikx}\left(\;\delta u^t(z),\quad \delta u^x(z),\quad 0,\quad \delta u^z(z)\;\right). \tag{5.13}$$

The other new fields are perturbed similarly,

$$n = n_0(z) + \varepsilon e^{-i\omega t+ikx}\delta n(z)\,, \tag{5.14}$$

$$\phi = \phi_0(z) + \varepsilon e^{-i\omega t+ikx}\delta\phi(z)\,, \tag{5.15}$$

$$\begin{aligned}\rho_{fl}(n) &= \rho_0(n_0(z)) + \varepsilon e^{-i\omega t+ikx}\frac{\partial\rho}{\partial n}\delta n(z)\\ &= \rho_0(z) + \varepsilon e^{-i\omega t+ikx}\mu_0\,\delta n(z)\,.\end{aligned} \tag{5.16}$$

The background equations of motion are changed into

$$(p_0+\rho_0)f' - 2\sqrt{f}n_0h' + 2fp' = 0\,, \tag{5.17}$$

$$4fg + fg^2(p_0+\rho_0)z^2 + gzf' + fzg' = 0\,, \tag{5.18}$$

$$-2f + 6fgz^2 + 2fgp_0z^2 + 2zf' - z^2\big(h'\big)^2 = 0\,, \tag{5.19}$$

$$-2\sqrt{f}gn_0 + z(p_0+\rho_0)gh' + 2h'' = 0\,, \tag{5.20}$$

and can no longer be solved analytically. The fluid Lagrangian introduces one additional ODE to solve for the perturbations; for $\delta\phi$ inside the cloud. The obtained perturbation equations of motion are lengthy, and are included in appendix A.

This inclusion of a possible charge density in the bulk is a natural next step for bottom-up models attempting to model real fermion systems better. It allows for a boundary theory with an additional two tune-able parameters, as well as a theoretically more sound description of low-temperature systems. This is the system considered in paper IV, as it naturally extends the work in paper I and III to include additional scales as well as being a mode of instability for those system towards lower temperatures (something that is very natural to study as superconductivity is achieved for small temperatures).

Most importantly, we find that this model retains the same takeaways as the RN-model - it does not eliminate the exotic transition, the strongly damped plasmon or the strong dependence on the dynamic metric.

The next thing we find is the introduction of a new mode to the system. This mode is also hydrodynamic and is intricately related to waves in the cloud. It starts off linearly, but experiences a similar exotic transition as the plasmon.

5.4 Breaking translational invariance

Another very natural extension of a holographic model, is to emulate the breaking of translational invariance in some form. In a metal, the material is not identical everywhere. Macroscopically, it can be, but on a microscopic level, there is a lattice structure that explicitly breaks the translation symmetry of the electron gas. It is therefore interesting to investigate what effects such breaking would have in a holographic model. There are several ways to do this, with a range of complexities. We opted for one of the simplest ones – an axion model that breaks the translation symmetries homogeneously. This means that although they are broken, they are broken identically everywhere. We get a rigidity to the system, but we don't get a lattice cell length. Although the rigidity is coupled to this length scale, it is less intuitive to compare to than a cell length which can be immediately compared to a wave length.

We leave the electron cloud model behind in favor of the less intricate RN-model, once again with action (4.6), and add to this an additional term,

$$\mathcal{L}_\phi = -\frac{1}{4}m^2 V(X)\,, \tag{5.21}$$

where m is the mass, $V(X)$ is a potential, and X is defined as $g^{\mu\nu}\partial_\mu\phi^I\partial_\nu\phi^I$, where $\phi^I\,, I = x, y$ are Stückelberg scalars. This setup once again allows for an analytic static background solution, similar to the one found in chapter 4. With a slightly optimized metric ansatz, setting L to unity,

$$\mathrm{d}s^2 = g_{\mu\nu}\,\mathrm{d}x^\mu x^\nu = -\frac{1}{z^2}\left(f(z)\,\mathrm{d}t^2 + \mathrm{d}x^2 + \mathrm{d}y^2 + \frac{1}{f(z)}\,\mathrm{d}z^2\right)\,, \tag{5.22}$$

we find, as before,

$$A_t = h(z) = Q(1-z)\,, \tag{5.23}$$

but also

$$f(z) = z^3 \int_z^1 \mathrm{d}v \left[\frac{3}{v^4} - \frac{m^2}{4v^4}V(v) - \frac{Q^2}{2}\right] \tag{5.24}$$

where $V(v)$ is to be read as $V(X)|_{z=v}$ and radially constant

$$\phi^I = \alpha\, x^I\,. \tag{5.25}$$

In this background, the chemical potential and charge density on the boundary are

$$\mu = \frac{Q}{\sqrt{\lambda}} r_H\,, \qquad \rho = \sqrt{\lambda} Q r_H^2\,, \tag{5.26}$$

and the temperature is

$$T = \frac{12 - m^2 V(1) - 2Q^2}{16\pi} r_h\,, \tag{5.27}$$

where once again $V(1)$ should be interpreted as $V(X)$ evaluated at the horizon, $z = 1$. Note how the background is now parameterized by two values, Q and α, but only the former appears in the holographic dictionary for the chemical potential and charge density, meaning this model does not solve the parameterization weaknesses that the electron cloud model did. The parameter α always appear together with factors of m. One can therefore without loss of generality set $m = 1$ and rescale α accordingly. The inclusion of one additional field implies one additional equation of motion to solve for, as well as alters the other equations of motion.

Depending on the choice of potential, one ends up with different types of translation breaking models. We opted to study two particular models that have been previously studied in other contexts. An identity potential, $V(X) = X$ corresponding to the linear axions model [71] which explicitly breaks translational invariance, and a cubic potential, $V(X) = X^3$ which instead spontaneously breaks translational invariance [72]. Functionally these are both interesting. Where the first one implements momentum losses to external media (which could be the lattice or defects in the specific situation) and the second one implements a sort of formation of internal rigidity to the plasma itself, necessary for phonons in the medium. The corresponding differential equations can be found in appendix A.3 and A.4.

These are the systems considered in paper V. Notably, we observe that the inclusion of explicit symmetry breaking shortens the relaxation time of the plasmon mode following an inverse Matthiessen's rule,

$$\tau_{total}^{-1} = \tau_{Coulomb}^{-1} + \tau_{SB}^{-1}\,. \tag{5.28}$$

The inclusion of explicit symmetry breaking also increases the value of the fitted plasma frequency, particularly at parameter values for which the plasmon mode is purely imaginary (diffusive). This would be a rather surprising result in a system with quasiparticles, as it would imply that the effective mass becomes smaller. In the strongly coupled system however, the same argument cannot be made. Instead, this is simply interpreted as that in a more rigid system, more energy is needed to excite the collective mode, a rather natural conclusion.

For the spontaneously broken translational symmetry, also considered in paper V, we make two important observations of how the behaviour of the model changes. Firstly, there is an additional (Goldstone) mode, as expected from this system [73], and secondly we observe a smooth transition from the typical fluid regime of the boundary theory into a more rigid "crystal" regime. This is most prominently seen in the speed of sound of modes, which transitions from its conformal value of $1/\sqrt{2}$, to the elastic 1. We also observe a competition behind the expected behaviour of a plasma oscillation (gapped) and the expected behaviour of a sound wave (linear) in the crystalline regime, which arguably is a rather healthy feature to have.

5.5 Transverse collective modes

Where our interest lies primarily in the longitudinal sector (the sector in which what is typically referred to as the plasmon exists), the separation between a longitudinal and a transverse sector is only truly possible for rather simple, isotropic systems. With the ultimate goal of describing plasmons seen in the lab, the transverse sector cannot be fully neglected. Common experimental setups include magnetic fields, which break the isotropy of systems and mixes the sectors.

Thankfully, treating the transverse sector is rather similar to the treatment of the longitudinal sector, with the additional advantage of significantly fewer fields and equations. The core is still to make sure that the boundary fields obey Maxwell's equations, and in particular Ampère's law (5.1). Following the same treatment as in section 5.1 this takes a similar form to the longitudinal sector (5.5). If we stick to the Reissner-Nordström model of chapter 4, or the expanded models of section 5.3 or 5.4, it simply becomes

$$\left(\left(\omega^2 - k^2\right)\delta A_y + \lambda \delta A_y'\right)\Big|_{z\to 0} = 0\,, \tag{5.29}$$

where k is still in the x-direction. That is, we once again do not want to impose Dirichlet boundary conditions, but rather this mixed condition.

We chose to consider transverse collective modes only in the models with momentum dissipation, which of course still includes the RN-metal as a special case, and our findings resulted in paper VI. Starting from this special case, we find the dispersion curves in the transverse sector and find that

they follow the expectations rather well, modulated similarly to the longitudinal dispersion relations due to the strongly coupled nature of the system. There is a slight difference in nature of how the gap of the "transverse plasmon" arises, due to how in the longitudinal sector, there is a sound mode it interacts with, whereas in the transverse sector there is only a diffusion mode which it doesn't interact with, simplifying the transition. This holds true until we also break translational invariance. With the symmetry explicitly broken, these modes starts to interact with each other, but unlike in the longitudinal case, here they repel, which does not affect the dispersion relations as much. With spontaneously broken translation symmetry, an additional mode appears, as expected, and interacts with the previously existing diffusion mode, instead giving rise to a translational sound mode.

5.6 Magnetic fields and broken parity

When conducting real experiments in the lab, it is a common scenario to have the material in an external magnetic field. This significantly affects the symmetries of the system, as the directions along or against the magnetic field lines are no longer equal, breaking parity invariance. In these systems, it is no longer possible to separate a longitudinal and a transverse sector.

As an extension of previous work however, the addition is quite straightforward. We consider the RN-metal of chapter 4 once again, but as we build primarily on the addition of the transverse sector, we stick with the conventions used in 5.4, simply without $\mathcal{L}_\phi$. In this model, the background gauge field is adjusted to include a magnetic field,

$$A_\mu = L \begin{pmatrix} h(z) & 0 & \mathcal{B}x & 0 \end{pmatrix}, \tag{5.30}$$

which results in an external magnetic field on the boundary,

$$B = \frac{\mathcal{B}}{\sqrt{\lambda} z_h^2}. \tag{5.31}$$

This means the black hole in the bulk is now truly a dyonic black hole, carrying both electric and magnetic charges. The emblackening factor reflects this,

$$f(z) = 1 - \left(\frac{z}{z_h}\right)^3 + \frac{1}{2}\left(\mathcal{B}^2 + Q^2\right)\left(\frac{z}{z_h}\right)^3 \left(\frac{z}{z_h} - 1\right), \tag{5.32}$$

and naturally, so does the temperature,

$$T = \frac{6 - \left(Q^2 + \mathcal{B}^2\right)}{8\pi z_h L}. \tag{5.33}$$

The next crucial step to incorporate Maxwell's equations on the boundary is once again to translate them into boundary conditions. In this setting,

it corresponds to implementing both boundary conditions (5.5) and (5.29) in the full boundary value matrix (4.33). The full system of 9 coupled differential equations needs to be solved, and the equations can be found in appendix A.5.

This is the system considered in VII, where we limit ourselves to consider neutral systems, where there exists excellent previous theoretical results from magnetohydrodynamics [55] which our results can be compared to, in the hydrodynamic limit. We find excellent agreement in this particular limit, but some rather important break downs as one considers modes further away from the origin in the (ω, k)-plane. Most significantly, we capture more modes, which further away from the small B-limit become increasingly important, something hydrodynamics cannot capture. Additionally, we find higher order corrections typically neglected in hydrodynamic treatments.

Chapter 6

Future Directions

In papers I-VII the dynamic charge response of strongly coupled matter is treated in terms bottom-up holography. Several significant properties are found, such as the strongly damped, gapped bulk plasmon in paper I, and the characteristic $\omega \propto \sqrt{k}$ dispersion of the 2D plasmon in paper II. Novel behaviour is discovered and discussed in paper III, that has not yet been accessible to experiments, and the robustness of these results through parameters space and different bulk models is observed in paper IV. In paper V, explicit and spontaneously broken translation symmetries are added to the system and studied. In the same symmetry broken phases, the transverse modes are studied in VI. And in VII, the experimentally relevant setup of including an external magnetic field is considered.

This might seem like a rather extensive search and expansion of the treatment of plasmons holographically, but there are still plenty of interesting questions to follow up in these papers. The most significant improvement of the results and usefulness of this framework is likely to consider better and more general models, a few of which I'd like to highlight here, as they've sparked enough interest to generate some additional research from myself.

Firstly, all the models considered so far in this thesis are bottom-up. Whereas these are advanced enough to include the necessary parts, the quantum consistency guaranteed from a top-down string theory model is very alluring. Secondly, the number of spatial dimensions in the boundary theory has so far been two, in contrast to the three we see in reality. Where the effects of this extra dimension for simpler systems are rather unimportant, the more advanced the model becomes, the less true this statement remains. For instance, in the case of a magnetic field in two dimensions, it effectively always points in the "third", i.e. always perpendicular to both transverse and longitudinal waves. In three dimensions however, this is clearly not the case, and to study any non-perpendicular angle between magnetic field and mode, the model would need an additional spatial dimension. Similar arguments can be made for any anisotropic system, and

in fact, high temperature superconductors such as the cuprates are often layered materials, i.e. explicitly anisotropic, even macroscopically.

Both these points lead us to develop an entirely new model, that of VIII. This model considers a bulk with a number of fully backreacted intersecting D5 and (black) D3-branes, with an additional probe D7-brane with a Dirac-Born-Infeld action. The D5-branes span two of the spatial boundary dimensions, and are smeared in the third resulting in a layered boundary theory. This is a quite intricate, but very powerful and flexible model, in which we studied the quasi-normal modes, but never got quite all the way to study plasmons. Taking the last step to include Coulomb interactions is work in progress, and some initial results can be found in this Master's thesis [74]. An alternative approach to layered materials, staying in the bottom-up picture, was carried out in [59].

Staying instead in the bottom-up picture, the most natural extension is the inclusion of one additional spatial dimension, moving to AdS_5. Where an odd number of dimensions provide some additional challenges, due to transcendental series and logarithmic divergences, this is by all means mathematical difficulties that can be overcome with some standard methods. When moving to AdS_5, another door opens, due to the possible anisotropy between directions, and that is the possible study of *surface plasmon polaritons*, which are some of the most commonly studied plasmons in the lab. These are collective excitations that live in the interface between a metal and the surrounding medium. Work on this is currently being made and some preliminary developments are available in this Master's thesis [75].

Another avenue worth pursuing are holographic superconductors. Previous work yielding holographic superconductors couple the bulk to an additional charged scalar field, and it would be interesting to treat those models with a proper dynamic charge response as in the paper I-IV. This is work in progress by Gran et al. and some initial work was presented in this Master's thesis [76].

Another improvement on the models considered above would be to consider an explicit lattice, i.e. not only break translations but actually include a periodic background potential. This significantly complicates things, immediately promoting ordinary differential equations into partial differential equations, with the additional problem of how exactly these potentials would look, but a possible starting point would be similar treatments as in [77–79].

There are also numerous experimental developments targeting strange metals that would be highly beneficial for these theoretical studies, as the experimental techniques that can probe these dynamic properties of strange metals have only been available the last few years. Apart from more experimental data in general, data especially near the novel behaviour found in III and IV would be of particular interest.

Bibliography

[1] M. Tornsö, *Holographic descriptions of collective modes in strongly correlated media.* Licentiate thesis, Chalmers University, Sept., 2019.

[2] H. Kamerlingh Onnes, *Further experiments with liquid helium. d. on the change of electric resistance of pure metals at very low temperatures, etc. v. the disappearance of the resistance of mercury.*, *Comm. Phys. Lab. Univ. Leiden* **No. 122b** (1911) .

[3] J. Bardeen, L. N. Cooper and J. R. Schrieffer, *Microscopic theory of superconductivity*, *Phys. Rev.* **106** (Apr, 1957) 162–164.

[4] J. G. Bednorz and K. A. Müller, *Possible high tc superconductivity in the ba-la-cu-o system*, *Zeitschrift für Physik B Condensed Matter* **64** (Jun, 1986) 189–193.

[5] R. Zia, J. A. Schuller, A. Chandran and M. L. Brongersma, *Plasmonics: the next chip-scale technology*, *Materials Today* **9** (2006) 20 – 27.

[6] W. L. Barnes, A. Dereux and T. W. Ebbesen, *Surface plasmon subwavelength optics*, *Nature* **424** (08, 2003) 824–830.

[7] F. Nugroho, I. Darmadi, L. Cusinato, A. Susarrey Arce, H. Schreuders, L. J. Bannenberg et al., *Metal–polymer hybrid nanomaterials for plasmonic ultrafast hydrogen detection*, *Nature Materials* (05, 2019) .

[8] F. H. L. Koppens, D. E. Chang and F. J. García de Abajo, *Graphene Plasmonics: A Platform for Strong Light-Matter Interactions*, *Nano Letters* **11** (Aug., 2011) 3370–3377, [1104.2068].

[9] T. Presbyter, *Schedula diversarum artium.* ca. 1100-1120.

[10] M. I. Stockman, *Nanoplasmonics: The physics behind the applications*, *Physics Today* **62 (2), 39** (2011) .

[11] I. Langmuir, *Oscillations in ionized gases*, *Proceedings of the National Academy of Sciences* **14** (1928) 627–637.

[12] D. Pines, *Collective energy losses in solids*, *Rev. Mod. Phys.* **28** (Jul, 1956) 184–198.

[13] S. Maier, *Plasmonics: Fundamentals and applications*. Springer US, 2007, 10.1007/0-387-37825-1.

[14] S. Szunerits and R. Boukherroub, *Introduction to Plasmonics: Advances and Applications*. Jenny Stanford Publishing, 2015, 10.1201/b18229.

[15] J. D. Jackson, *Classical electrodynamics*. Wiley, 1975.

[16] D. Pines and P. Nozières, *The Theory of Quantum Liquids*. W.A. Benjamin Inc., 1966.

[17] J. D. Jackson, *From Lorenz to Coulomb and other explicit gauge transformations*, *Am. J. Phys.* **70** (2002) 917–928, [physics/0204034].

[18] B. M. Santoyo and M. del Castillo-Mussot, *Plasmons in three, two and one dimension*, *Rev. Mex. Física* **4** (1993) 640–652.

[19] M. Müller and S. Sachdev, *Collective cyclotron motion of the relativistic plasma in graphene*, *Phys. Rev.* **B78** (2008) 115419, [0801.2970].

[20] E. H. Hwang and S. Das Sarma, *Dielectric function, screening, and plasmons in two-dimensional graphene*, *Phys. Rev. B* **75** (May, 2007) 205418.

[21] B. Wunsch, T. Stauber, F. Sols and F. Guinea, *Dynamical polarization of graphene at finite doping*, *New Journal of Physics* **8** (dec, 2006) 318–318.

[22] Y. Liu and R. F. Willis, *Plasmon-phonon strongly coupled mode in epitaxial graphene*, *Phys. Rev. B* **81** (Feb, 2010) 081406.

[23] Z. Fei, G. O. Andreev, W. Bao, L. M. Zhang, A. S. McLeod, C. Wang et al., *Infrared nanoscopy of dirac plasmons at the graphene–sio2 interface*, *Nano Letters* **11** (2011) 4701–4705.

[24] V. W. Brar, M. S. Jang, M. Sherrott, S. Kim, J. J. Lopez, L. B. Kim et al., *Hybrid surface-phonon-plasmon polariton modes in graphene/monolayer h-bn heterostructures*, *Nano Letters* **14** (2014) 3876–3880.

[25] M. Mitrano, A. A. Husain, S. Vig, A. Kogar, M. S. Rak, S. I. Rubeck et al., *Anomalous density fluctuations in a strange metal*, *Proceedings of the National Academy of Sciences* **115** (May, 2018) 5392–5396.

[26] A. A. Husain, M. Mitrano, M. S. Rak, S. Rubeck, B. Uchoa, K. March et al., *Crossover of charge fluctuations across the strange metal phase diagram*, *Physical Review X* **9** (Dec, 2019) .

[27] H. Schulz, *Fermi liquids and non-fermi liquids*, in *Proceedings of Les Houches Summer School LXI*, (Elsevier, Amsterdam), 1995. [cond-mat/9503150].

[28] S. A. Hartnoll, J. Polchinski, E. Silverstein and D. Tong, *Towards strange metallic holography*, *JHEP* **04** (2010) 120, [0912.1061].

[29] O. Bergman, N. Jokela, G. Lifschytz and M. Lippert, *Quantum Hall Effect in a Holographic Model*, *JHEP* **10** (2010) 063, [1003.4965].

[30] N. Jokela, G. Lifschytz and M. Lippert, *Magneto-roton excitation in a holographic quantum Hall fluid*, *JHEP* **02** (2011) 104, [1012.1230].

[31] J. Crossno, J. K. Shi, K. Wang, X. Liu, A. Harzheim, A. Lucas et al., *Observation of the Dirac fluid and the breakdown of the Wiedemann-Franz law in graphene*, *Science* **351** (Mar., 2016) 1058–1061, [1509.04713].

[32] B. Keimer, S. A Kivelson, M. R Norman, S. Uchida and J. Zaanen, *From quantum matter to high-temperature superconductivity in copper oxides*, *Nature* **518** (02, 2015) 179–86.

[33] A. Legros, S. Benhabib, W. Tabis, F. Laliberté, M. Dion, M. Lizaire et al., *Universal T-linear resistivity and Planckian dissipation in overdoped cuprates*, *Nature Physics* **15** (Nov, 2018) 142–147, [1805.02512].

[34] P. R. Wallace, *The Band Theory of Graphite*, *Phys. Rev.* **71 (622)** (1947) .

[35] A. Lucas, J. Crossno, K. C. Fong, P. Kim and S. Sachdev, *Transport in inhomogeneous quantum critical fluids and in the Dirac fluid in graphene*, *Phys. Rev. B* **93** (2016) 075426, [1510.01738].

[36] S. Hartnoll, A. Lucas and S. Sachdev, *Holographic Quantum Matter*. MIT Press, 2018, [1612.07324].

[37] J. Zaanen, Y.-W. Sun, Y. Liu and K. Schalm, *Holographic Duality in Condensed Matter Physics*. Cambridge University Press, 2015.

[38] M. Ammon and J. Erdmenger, *Gauge/gravity duality*. Cambridge University Press, 2015.

[39] J. M. Maldacena, *The Large N limit of superconformal field theories and supergravity*, *Int. J. Theor. Phys.* **38** (1999) 1113–1133, [hep-th/9711200].

[40] G. Policastro, D. T. Son and A. O. Starinets, *The Shear viscosity of strongly coupled N=4 supersymmetric Yang-Mills plasma*, *Phys. Rev. Lett.* **87** (2001) 081601, [hep-th/0104066].

[41] D. Marolf, W. Kelly and S. Fischetti, *Conserved Charges in Asymptotically (Locally) AdS Spacetimes*, in *Springer Handbook of Spacetime* (A. Ashtekar and V. Petkov, eds.), pp. 381–407. Springer, 2014. [1211.6347]. 10.1007/978-3-642-41992-8_19.

[42] J. M. Martín-García, *xAct: Efficient tensor computer algebra for the wolfram language*, https://www.xact.es, Accessed 2019-01-01.

[43] T. Nutma, *xTras : A field-theory inspired xAct package for mathematica*, *Comput. Phys. Commun.* **185** (2014) 1719–1738, [1308.3493].

[44] I. Amado, M. Kaminski and K. Landsteiner, *Hydrodynamics of Holographic Superconductors*, *JHEP* **05** (2009) 021, [0903.2209].

[45] M. Edalati, J. I. Jottar and R. G. Leigh, *Holography and the sound of criticality*, *JHEP* **10** (2010) 058, [1005.4075].

[46] R. A. Davison and N. K. Kaplis, *Bosonic excitations of the AdS_4 Reissner-Nordstrom black hole*, *JHEP* **12** (2011) 037, [1111.0660].

[47] B. Wang, C.-Y. Lin and E. Abdalla, *Quasinormal modes of Reissner-Nordstrom anti-de Sitter black holes*, *Phys. Lett.* **B481** (2000) 79–88, [hep-th/0003295].

[48] E. Berti and K. D. Kokkotas, *Quasinormal modes of Reissner-Nordstrom-anti-de Sitter black holes: Scalar, electromagnetic and gravitational perturbations*, *Phys. Rev.* **D67** (2003) 064020, [gr-qc/0301052].

[49] A. Amariti, D. Forcella, A. Mariotti and G. Policastro, *Holographic Optics and Negative Refractive Index*, *JHEP* **04** (2011) 036, [1006.5714].

[50] L. Liu and H. Liu, *Wake potential in a strong coupling plasma from the AdS/CFT correspondence*, *Phys. Rev.* **D93** (2016) 085011, [1502.01841].

[51] G. Mahan, *Many-Particle Physics*. Physics of Solids and Liquids. Springer US, 2000.

[52] P. Kovtun, D. T. Son and A. O. Starinets, *Viscosity in strongly interacting quantum field theories from black hole physics*, *Phys. Rev. Lett.* **94** (2005) 111601, [hep-th/0405231].

[53] G. Policastro, D. T. Son and A. O. Starinets, *From AdS / CFT correspondence to hydrodynamics*, *JHEP* **09** (2002) 043, [hep-th/0205052].

[54] S. Bhattacharyya, V. E. Hubeny, S. Minwalla and M. Rangamani, *Nonlinear Fluid Dynamics from Gravity*, *JHEP* **02** (2008) 045, [0712.2456].

[55] J. Hernandez and P. Kovtun, *Relativistic magnetohydrodynamics*, *JHEP* **05** (2017) 001, [1703.08757].

[56] E. Witten, *Multitrace operators, boundary conditions, and AdS / CFT correspondence*, hep-th/0112258.

[57] W. Mueck, *An Improved correspondence formula for AdS / CFT with multitrace operators*, *Phys. Lett.* **B531** (2002) 301–304, [hep-th/0201100].

[58] M. Ihl, N. Jokela and T. Zingg, *Holographic anyonization: A systematic approach*, *JHEP* **06** (2016) 076, [1603.09317].

[59] E. Mauri and H. T. C. Stoof, *Screening of Coulomb interactions in Holography*, *JHEP* **04** (2019) 035, [1811.11795].

[60] A. Romero-Bermúdez, A. Krikun, K. Schalm and J. Zaanen, *Anomalous attenuation of plasmons in strange metals and holography*, *Phys. Rev. B* **99** (2019) 235149, [1812.03968].

[61] A. Lucas and K. C. Fong, *Hydrodynamics of electrons in graphene*, *J. Phys. Condens. Matter* **30** (2018) 053001, [1710.08425].

[62] A. Lucas and S. Das Sarma, *Electronic sound modes and plasmons in hydrodynamic two-dimensional metals*, *Physical Review B* **97** (Mar, 2018) 115449, [1801.01495].

[63] J. Lucietti, K. Murata, H. S. Reall and N. Tanahashi, *On the horizon instability of an extreme Reissner-Nordström black hole*, *JHEP* **03** (2013) 035, [1212.2557].

[64] S. Aretakis, *Stability and Instability of Extreme Reissner-Nordström Black Hole Spacetimes for Linear Scalar Perturbations I*, *Commun. Math. Phys.* **307** (2011) 17–63, [1110.2007].

[65] S. Aretakis, *Stability and Instability of Extreme Reissner-Nordstrom Black Hole Spacetimes for Linear Scalar Perturbations II*, *Annales Henri Poincare* **12** (2011) 1491–1538, [1110.2009].

[66] S. A. Hartnoll, C. P. Herzog and G. T. Horowitz, *Building a Holographic Superconductor*, *Phys. Rev. Lett.* **101** (2008) 031601, [0803.3295].

[67] S. A. Hartnoll, C. P. Herzog and G. T. Horowitz, *Holographic Superconductors*, *JHEP* **12** (2008) 015, [0810.1563].

[68] V. G. M. Puletti, S. Nowling, L. Thorlacius and T. Zingg, *Holographic metals at finite temperature*, *JHEP* **01** (2011) 117, [1011.6261].

[69] S. A. Hartnoll and A. Tavanfar, *Electron stars for holographic metallic criticality*, *Phys. Rev.* **D83** (2011) 046003, [1008.2828].

[70] R. Amorim, *Charged spinning fluids in general relativity*, *Physics Letters A* **104** (1984) 259–261.

[71] T. Andrade and B. Withers, *A simple holographic model of momentum relaxation*, *JHEP* **05** (2014) 101, [1311.5157].

[72] L. Alberte, M. Ammon, A. Jiménez-Alba, M. Baggioli and O. Pujolàs, *Holographic Phonons*, *Phys. Rev. Lett.* **120** (2018) 171602, [1711.03100].

[73] T. Andrade, M. Baggioli, A. Krikun and N. Poovuttikul, *Pinning of longitudinal phonons in holographic spontaneous helices*, *JHEP* **02** (2018) 085, [1708.08306].

[74] O. Lexell, *A top-down model for layered holographic strange metals*, Master's thesis, Chalmers University, 2021.

[75] E. Nilsson, *Surface plasmon polaritons in strongly correlated media*, Master's thesis, Chalmers University, 2021.

[76] M. Lassila, *Holographic duality and strongly interacting quantum matter*, Master's thesis, Chalmers University, 2020.

[77] T. Andrade, A. Krikun, K. Schalm and J. Zaanen, *Doping the holographic Mott insulator*, *Nature Phys.* **14** (2018) 1049–1055, [1710.05791].

[78] F. Balm, A. Krikun, A. Romero-Bermúdez, K. Schalm and J. Zaanen, *Isolated zeros destroy Fermi surface in holographic models with a lattice*, *JHEP* **01** (2020) 151, [1909.09394].

[79] A. Donos, J. P. Gauntlett and C. Pantelidou, *Holographic Abrikosov Lattices*, *JHEP* **07** (2020) 095, [2001.11510].

Appendix A

Perturbation equations

In the following sections are the equations of motion for the perturbations in the models used.

A.1 Equations of motion: EC, and RN

These are the equations of motion for the electron cloud bulk model. The equations of motion for the Reissner-Nordström bulk model are similar, and obtained by letting $\sigma, \rho \to 0$.

δA_t-variation equation:

$$\delta A_t'' + \left(-\frac{f'}{2f} - \frac{g'}{2g} - \frac{2}{z}\right)\delta A_t' + \frac{g\left(2f^{3/2}\sigma' - hk^2z^2f' + 2fk^2z^2h'\right)}{hf' - 2fh'}\delta A_t + \frac{h'}{2f}\delta g_{tt}' - gk\omega z^2\delta A_x + \frac{1}{2}z^2\delta g_{xx}'h' + zh'\delta g_{xx} + \frac{1}{2}z^2h'\delta g_{yy}' + zh'\delta g_{yy} + \frac{2if^{3/2}g\omega\sigma'}{2fh' - hf'}\delta\phi + \left(-f^{3/2}g\sigma - 2f'h' + \frac{2f^{5/2}gh\sigma'}{hf' - 2fh'} + f\left(2h'' - h'\left(\frac{g'}{g} + \frac{4}{z}\right)\right)\right)\frac{\delta g_{tt}}{2f^2} = 0$$

δA_x-variation equation:

$$\delta A_x'' + \frac{gk\omega}{f}\delta A_t + \frac{1}{2}\left(\frac{f'}{f} - \frac{g'}{g}\right)\delta A_x' + \frac{g\left(\omega^2 - \frac{f^{3/2}\sigma}{h}\right)}{f}\delta A_x + \frac{h'}{f}\delta g_{tx}' - \frac{\left(2f^{3/2}g^2\sigma + gf'h' + fg'h' - 2fgh''\right)}{2f^2g}\delta g_{tx} - \frac{ik\sqrt{f}g\sigma}{h}\delta\phi = 0$$

δA_y-variation equation:

$$\delta A_y'' + \frac{\delta A_y'\left(gf' - fg'\right)}{2fg} + \frac{\delta A_y\left(-f^{3/2}g\sigma - fghk^2z^2 + gh\omega^2\right)}{fh} + \frac{\delta g_{ty}'h'}{f} + \frac{\delta g_{ty}\left(-2f^{3/2}g^2\sigma - gf'h' - fg'h' + 2fgh''\right)}{2f^2g} = 0$$

$\delta\phi$-equation, from n-variation:

$$\delta\phi'' + \delta\phi'\left(\frac{f'}{f} - \frac{g'}{2g} - \frac{h'}{h} + \frac{\sigma'}{\sigma} - \frac{2}{z}\right) + \delta\phi g\left(-\frac{2h\omega^2\sigma'}{h\sigma f' - 2f\sigma h'} - k^2z^2\right) + \frac{i\delta g_{tx}ghkz^2}{f} + \frac{i\delta g_{xx}gh\omega z^2}{2f} + \frac{i\delta g_{yy}gh\omega z^2}{2f} - \frac{2i\delta A_t gh\omega\sigma'}{h\sigma f' - 2f\sigma h'} + i\delta A_x gkz^2 - \frac{i\delta g_{tt}gh^2\omega\sigma'}{fh\sigma f' - 2f^2\sigma h'} = 0$$

δg_{tt}-variation equation:

$$\delta g_{tt}'' + \left(-\frac{f'}{f} - \frac{g'}{2g} - \frac{1}{z}\right)\delta g_{tt}' + 3h'\delta A_t' + \frac{2\sqrt{f}g\left(h\left(f\sigma' - \sigma f'\right) + 2f\sigma h'\right)}{2fh' - hf'}\delta A_t - gk\omega z^2\delta g_{tx} - \frac{1}{4}\left(z^2f\right)'\left(\delta g_{xx}' + \delta g_{yy}'\right) + \frac{2i\omega\sqrt{f}g\left(h\left(f\sigma' - \sigma f'\right) + 2f\sigma h'\right)}{hf' - 2fh'}\delta\phi + \frac{1}{f^2z^2}\left(\frac{fg'z\left(zf' + 2f\right)}{2g} + gf^2z^2\left(\frac{\sqrt{f}h^2\sigma'}{2fh' - hf'} + \frac{h\sigma}{\sqrt{f}} - \frac{k^2z^2}{2} + \rho - 3\right) + 5f^2 + z^2\left(f'\right)^2 + fz\left(-zf'' + f' + 2z\left(h'\right)^2\right)\right)\delta g_{tt} - \frac{1}{4fg}\left(4f^{3/2}g^2h\sigma z^2 + 2f^2\left(g^2z^2(-2\rho + 6) - zg' - 2g\right) + gz^2\left(f'\right)^2 + fz\left(zf'g' + 2g\left(-zf'' + 2f' + z\left(h'\right)^2\right) + 2g^2\omega^2z\right)\right)\delta g_{xx} - \frac{1}{4fg}\left(4f^{3/2}g^2h\sigma z^2 + 2f^2\left(g^2z^2\left(k^2z^2 - 2\rho + 6\right) - zg' - 2g\right) + gz^2\left(f'\right)^2 + fz\left(zf'g' + 2g\left(-zf'' + 2f' + z\left(h'\right)^2\right) + 2g^2\omega^2z\right)\right)\delta g_{yy} = 0$$

δg_{tx}-variation equation:

$$\delta g_{tx}'' + \left(-\frac{f'}{2f} - \frac{g'}{2g}\right)\delta g_{tx}' + \left(\frac{-zf' + 4f + z^2\left(h'\right)^2}{fz^2} + \frac{g'}{gz} + 2g(\rho - 3)\right)\delta g_{tx} + 2h'\delta A_x' + 2\sqrt{f}g\sigma\delta A_x + gk\omega z^2\delta g_{yy} + 2ik\sqrt{f}g\sigma\delta\phi = 0$$

δg_{ty}-variation equation:

$$\delta g_{ty}'' - \frac{\left(gf' + fg'\right)}{2fg}\delta g_{ty}' + \left(-\frac{f'}{fz} + \frac{\left(h'\right)^2}{f} + \frac{g'}{gz} - gk^2z^2 + 2g\rho - 6g + \frac{4}{z^2}\right)\delta g_{ty} + 2h'\delta A_y' + 2\sqrt{f}g\sigma\delta A_y - gk\omega z^2\delta g_{xy} = 0$$

δg_{xy}-variation equation:

$$\delta g''_{xy} + \frac{\delta g'_{xy}\left(gzf' - fzg' + 4fg\right)}{2fgz} + \frac{\delta g_{ty} gk\omega}{f}$$
$$+ \delta g_{xy}\left(\frac{f''}{f} - \frac{f'g'}{2fg} - \frac{(f')^2}{2f^2} - \frac{2gh\sigma}{\sqrt{f}} + \frac{g\omega^2}{f} - \frac{(h')^2}{f} + 2g\rho - 6g + \frac{2}{z^2}\right) = 0$$

δg_{yy}-variation equation:

$$\delta g''_{yy} + \frac{1}{4}\left(\frac{f'}{f} - \frac{2g'}{g} + \frac{6}{z}\right)\delta g'_{yy} + \left(-\frac{f'}{4f} - \frac{1}{2z}\right)\delta g'_{xx} - \frac{gk\omega}{f}\delta g_{tx}$$
$$+ \frac{h'}{fz^2}\delta A'_t - \frac{2\sqrt{f}gh\sigma'}{z^2\left(hf' - 2fh'\right)}\delta A_t + \frac{2i\omega\sqrt{f}gh\sigma'}{z^2\left(hf' - 2fh'\right)}\delta\phi$$
$$+ \frac{1}{2fz^2}\left(\frac{2(h')^2}{f} + \frac{2g'}{gz} + g\left(-k^2z^2 + 2\rho - 6\right) + \frac{10}{z^2} - \frac{2\sqrt{f}gh^2\sigma'}{hf' - 2fh'}\right)\delta g_{tt}$$
$$+ \frac{1}{4f^2gz^2}\Bigg(4f^{3/2}g^2h\sigma z^2 - 2f^2\left(2g^2(\rho-3)z^2 + zg' + 6g\right)$$
$$+ gz^2(f')^2 + fz^2\left(2g\left((h')^2 - f''\right) + f'g' - 2g^2\omega^2\right)\Bigg)\delta g_{xx}$$
$$- \frac{1}{4f^2gz^2}\Bigg(4f^{3/2}g^2h\sigma z^2 + 2f^2\left(g^2z^2\left(k^2z^2 - 2\rho + 6\right) + zg' + 2g\right)$$
$$+ gz^2(f')^2 + fz^2\left(2g\left((h')^2 - f''\right) + f'g' - 2g^2\omega^2\right)\Bigg)\delta g_{yy} = 0$$

δg_{xx}-variation equation:

$$\delta g''_{xx} + \frac{1}{4}\delta g'_{xx}\left(\frac{f'}{f} - \frac{2g'}{g} + \frac{6}{z}\right) + \delta g'_{yy}\left(-\frac{f'}{4f} - \frac{1}{2z}\right) + \frac{\delta A'_t h'}{fz^2} + \frac{\delta A_t gh\sigma'}{fz^2\mu'}$$
$$+ \frac{\delta g_{tt}}{2fz^2}\left(\frac{2(h')^2}{f} + \frac{2g'}{gz} + g\left(k^2z^2 + 2\rho - 6\right) + \frac{10}{z^2} - \frac{2\sqrt{f}gh^2\sigma'}{hf' - 2fh'}\right)$$
$$+ \delta g_{xx}\left(\frac{f''}{2f} - \frac{f'g'}{4fg} - \frac{(f')^2}{4f^2} - \frac{gh\sigma}{\sqrt{f}} + \frac{g\omega^2}{2f} - \frac{(h')^2}{2f} - \frac{g'}{2gz} + g\rho - 3g - \frac{1}{z^2}\right)$$
$$+ \frac{\delta g_{tx} gk\omega}{f} - \frac{i\delta\phi gh\omega\sigma'}{fz^2\mu'} + \delta g_{yy}\Bigg(-\frac{f''}{2f} + \frac{f'g'}{4fg} + \frac{(f')^2}{4f^2}$$
$$+ \frac{gh\sigma}{\sqrt{f}} - \frac{g\omega^2}{2f} + \frac{(h')^2}{2f} - \frac{g'}{2gz} - \frac{1}{2}gk^2z^2 - g\rho + 3g - \frac{3}{z^2}\Bigg) = 0$$

A.2 Constraint equations: EC and RN

These are the constraint equations for the electron cloud bulk model. These are satisfied by solutions to the equations of motion above. The constraints for the Reissner-Nordström bulk model are similar, and obtained by letting $\sigma, \rho \to 0$.

δg_{tz}-variation, constraint equation:

$$kz^2\delta g'_{tx} - \frac{\delta g_{tx} k z^2 f'}{f} + \omega z^2\left(\delta g'_{xx} + \delta g'_{yy}\right) + \omega z\left(1 - \frac{zf'}{2f}\right)\left(\delta g_{xx} + \delta g_{yy}\right) + 2i\sqrt{f}\sigma\delta\phi' = 0$$

δg_{xz}-variation, constraint equation:

$$2\delta A_t k z^2 h' + 2\delta A_x \omega z^2 h' + k z^2 \delta g'_{tt} + \delta g_{tt} k z\left(1 - \frac{zf'}{2f}\right) + \omega z^2 \delta g'_{tx} + 2\delta g_{tx}\omega z - f k z^4 \delta g'_{yy} - 2\delta g_{yy} f k z^3 = 0$$

δg_{yz}-variation, constraint equation:

$$2\omega h'\delta A_y + \omega\delta g'_{ty} + \frac{2\omega}{z}\delta g_{ty} + f k z^2 \delta g'_{xy} + 2 f k z \delta g_{xy} = 0$$

δg_{zz}-variation, constraint equation:

$$\begin{aligned} &4f\delta A'_t h' - 4\delta A_t f^{3/2} g\sigma + \frac{4f\delta g'_{tt}}{z} + 2\delta g_{tt}\left(-\frac{2f'}{z} - \sqrt{f}gh\sigma + fgk^2z^2 + \left(h'\right)^2\right) \\ &- fz\delta g'_{yy}\left(2f - zf'\right) - fz\delta g'_{xx}\left(2f - zf'\right) - 2\delta g_{xx} f\left(2f - zf' - g\omega^2 z^2\right) \\ &+ 4\delta g_{tx} f g k \omega z^2 - 2\delta g_{yy} f\left(fgk^2z^4 + 2f - zf' - g\omega^2 z^2\right) + 4i\delta\phi f^{3/2} g\omega\sigma = 0 \end{aligned}$$

δA_z-variation, constraint equation:

$$\omega\delta A'_t + f k z^2 \delta A'_x + \frac{\delta g_{tt}\omega h'}{2f} + \delta g_{tx} k z^2 h' + \frac{1}{2}\delta g_{xx}\omega z^2 h' + \frac{1}{2}\delta g_{yy}\omega z^2 h' - \frac{i f^{3/2}\sigma\delta\phi'}{h} = 0$$

A.3 Equations of motion: linear axions

These are the perturbation equations of motion for the linear axions potential $V(X) = X$ of section 5.4.

δg_{tt}-variation equation:

$$\frac{-6f^2+f\left(-z^2f''+4zf'+z^4\left(h'\right)^2+k^2z^2+\frac{1}{2}\alpha^2z^2+6\right)+\omega^2z^2}{2f^2z^2}\delta g_{yy}$$
$$+\frac{k\omega}{f^2}\delta g_{tx}+\frac{\left(-2zf'+6f+4z^4\left(h'\right)^2-k^2z^2+\alpha^2z^2-6\right)}{2fz^2}\delta g_{tt}$$
$$+\frac{\left(-12f^2+f\left(-2z^2f''+8zf'+2z^4\left(h'\right)^2+\alpha^2z^2+12\right)+2\omega^2z^2\right)}{4f^2z^2}\delta g_{xx}$$
$$+\left(\frac{3f'}{2f}-\frac{2}{z}\right)\delta g'_{tt}+\frac{f'}{4f}\delta g'_{xx}+\frac{f'}{4f}\delta g'_{yy}-\frac{3z^2h'}{f}\delta A'_t-\frac{i\alpha k}{2f}\delta\phi_x+\delta g''_{tt}=0$$

δg_{tx}-variation equation:

$$\frac{\left(-2zf'+6f+z^4\left(h'\right)^2-6\right)}{fz^2}\delta g_{tx}+\frac{k\omega}{f}\delta g_{yy}-\frac{i\alpha\omega}{f}\delta\phi_x$$
$$+2z^2h'\delta A'_x-\frac{2}{z}\delta g'_{tx}+\delta g''_{tx}=0$$

δg_{xx}-variation equation:

$$\frac{-6f^2+f\left(-z^2f''+4zf'+z^4\left(h'\right)^2-k^2z^2+\frac{1}{2}\alpha^2z^2+6\right)-\omega^2z^2}{2f^2z^2}\delta g_{yy}$$
$$+\frac{k\omega}{f^2}\delta g_{tx}-\frac{\left(-2zf'+6f+2z^4\left(h'\right)^2+k^2z^2+\alpha^2z^2-6\right)}{2fz^2}\delta g_{tt}$$
$$+\frac{\left(12f^2-f\left(-2z^2f''+8zf'+2z^4\left(h'\right)^2+3\alpha^2z^2+12\right)+2\omega^2z^2\right)}{4f^2z^2}\delta g_{xx}$$
$$+\frac{3i\alpha k}{2f}\delta\phi_x-\frac{f'\delta g'_{yy}}{4f}+\left(\frac{3f'}{4f}-\frac{2}{z}\right)\delta g'_{xx}+\delta g''_{xx}=0$$

δg_{yy}-variation equation:

$$\frac{6f^2-f\left(-z^2f''+4zf'+z^4\left(h'\right)^2+k^2z^2+\frac{3}{2}\alpha^2z^2+6\right)+\omega^2z^2}{2f^2z^2}\delta g_{yy}$$
$$-\frac{k\omega}{f^2}\delta g_{tx}+\frac{\left(2zf'-6f-2z^4\left(h'\right)^2+k^2z^2-\alpha^2z^2+6\right)}{2fz^2}\delta g_{tt}$$
$$+\frac{\left(-12f^2+f\left(-2z^2f''+8zf'+2z^4\left(h'\right)^2+\alpha^2z^2+12\right)-2\omega^2z^2\right)}{4f^2z^2}\delta g_{xx}$$
$$+\frac{z^2h'}{f}\delta A'_t-\frac{i\alpha k}{2f}\delta\phi_x-\frac{f'}{4f}\delta g'_{xx}+\left(\frac{3f'}{4f}-\frac{2}{z}\right)\delta g'_{yy}+\delta g''_{yy}=0$$

δA_t-variation equation:

$$-\frac{k^2}{f}\delta A_t - \frac{k\omega}{f}\delta A_x - \frac{1}{2}h'\delta g'_{tt} + \frac{1}{2}h'\delta g'_{xx} + \frac{1}{2}h'\delta g'_{yy} + \delta A''_t = 0$$

δA_x-variation equation:

$$\frac{k\omega}{f^2}\delta A_t + \frac{\omega^2}{f^2}\delta A_x + \frac{f'}{f}\delta A'_x + \frac{h'}{f}\delta g'_{tx} + \delta A''_x = 0$$

$\delta\phi_x$-variation equation:

$$\frac{i\alpha k}{2f}\delta g_{tt} - \frac{i\alpha\omega}{f^2}\delta g_{tx} - \frac{i\alpha k}{2f}\delta g_{xx} + \frac{i\alpha k}{2f}\delta g_{yy} + \frac{\left(\omega^2 - fk^2\right)}{f^2}\delta\phi_x + \left(\frac{f'}{f} - \frac{2}{z}\right)\delta\phi'_x + \delta\phi''_x = 0$$

δg_{ty}-variation equation:

$$\frac{\left(-2zf' + 6f - k^2z^2 + Q^2z^4 - 6\right)}{z^2 f}\delta g_{ty} - \frac{k\omega}{f}\delta g_{xy} - \frac{i\alpha\omega}{f}\delta\phi_y - 2Qz^2\delta A'_y - \frac{2}{z}\delta g'_{ty} + \delta g''_{ty} = 0$$

δg_{xy}-variation equation:

$$\frac{\left(6f^2 - f\left(-z^2f'' + 4zf' + Q^2z^4 + \alpha^2z^2 + 6\right) + \omega^2z^2\right)}{f^2z^2}\delta g_{xy} + \frac{i\alpha k}{f}\delta\phi_y + \frac{k\omega}{f^2}\delta g_{ty} + \left(\frac{f'}{f} - \frac{2}{z}\right)\delta g'_{xy} + \delta g''_{xy} = 0$$

δA_y-variation equation:

$$\frac{\left(\omega^2 - fk^2\right)}{f^2}\delta A_y + \frac{f'}{f}\delta A'_y - \frac{Q}{f}\delta g'_{ty} + \delta A''_y = 0$$

$\delta\phi_y$-variation equation:

$$\frac{\left(\omega^2 - fk^2\right)}{f^2}\delta\phi_y - \frac{i\alpha\omega}{f^2}\delta g_{ty} - \frac{i\alpha k}{f}\delta g_{xy} + \left(\frac{f'}{f} - \frac{2}{z}\right)\delta\phi'_y + \delta\phi''_y = 0$$

A.4 Equations of motion: Cubic potential

These are the perturbation equations of motion for the cubic potential $V(X) = X^3$ of section 5.4.

δg_{tt}-variation equation:

$$\frac{-6f^2+f\left(-z^2f''+4zf'+z^4\left(h'\right)^2+k^2z^2+38\alpha^6z^6+6\right)+\omega^2z^2}{2f^2z^2}\delta g_{yy}$$
$$+\frac{k\omega}{f^2}\delta g_{tx}-\frac{\left(2zf'-6f-4z^4\left(h'\right)^2+k^2z^2-4\alpha^6z^6+6\right)}{2fz^2}\delta g_{tt}$$
$$+\frac{\left(-6f^2+f\left(-z^2f''+4zf'+z^4\left(h'\right)^2+38\alpha^6z^6+6\right)+\omega^2z^2\right)}{2f^2z^2}\delta g_{xx}$$
$$+\left(\frac{3f'}{2f}-\frac{2}{z}\right)\delta g'_{tt}+\frac{f'}{4f}\delta g'_{xx}+\frac{f'}{4f}\delta g'_{yy}-\frac{3z^2h'}{f}\delta A'_t-\frac{30i\alpha^5kz^4}{f}\delta\phi_x+\delta g''_{tt}=0$$

δg_{tx}-variation equation:

$$\frac{\left(-2zf'+6f+z^4\left(h'\right)^2-8\alpha^6z^6-6\right)}{fz^2}\delta g_{tx}+\frac{k\omega}{f}\delta g_{yy}-\frac{12i\alpha^5\omega z^4}{f}\delta\phi_x$$
$$+2z^2h'\delta A'_x-\frac{2}{z}\delta g'_{tx}+\delta g''_{tx}=0$$

δg_{xx}-variation equation:

$$\frac{-6f^2+f\left(-z^2f''+4zf'+z^4\left(h'\right)^2-k^2z^2+14\alpha^6z^6+6\right)-\omega^2z^2}{2f^2z^2}\delta g_{yy}$$
$$+\frac{k\omega}{f^2}\delta g_{tx}-\frac{\left(-2zf'+6f+2z^4\left(h'\right)^2+k^2z^2+4\alpha^6z^6-6\right)}{2fz^2}\delta g_{tt}$$
$$+\frac{\left(6f^2-f\left(-z^2f''+4zf'+z^4\left(h'\right)^2+26\alpha^6z^6+6\right)+\omega^2z^2\right)}{2f^2z^2}\delta g_{xx}$$
$$+\frac{18i\alpha^5kz^4}{f}\delta\phi_x+\left(\frac{3f'}{4f}-\frac{2}{z}\right)\delta g'_{xx}-\frac{f'}{4f}\delta g'_{yy}+\frac{z^2h'}{f}\delta A'_t+\delta g''_{xx}=0$$

δg_{yy}-variation equation:

$$\frac{\left(6f^2-f\left(-z^2f''+4zf'+z^4\left(h'\right)^2+k^2z^2+26\alpha^6z^6+6\right)+\omega^2z^2\right)}{2f^2z^2}\delta g_{yy}$$
$$-\frac{k\omega}{f^2}\delta g_{tx}+\frac{\left(2zf'-6f-2z^4\left(h'\right)^2+k^2z^2-4\alpha^6z^6+6\right)}{2fz^2}\delta g_{tt}$$
$$+\frac{\left(-6f^2+f\left(-z^2f''+4zf'+z^4\left(h'\right)^2+14\alpha^6z^6+6\right)-\omega^2z^2\right)}{2f^2z^2}\delta g_{xx}$$
$$-\frac{6i\alpha^5kz^4}{f}\delta\phi_x-\frac{f'}{4f}\delta g'_{xx}+\left(\frac{3f'}{4f}-\frac{2}{z}\right)\delta g'_{yy}+\frac{z^2h'}{f}\delta A'_t+\delta g''_{yy}=0$$

δA_t-variation equation:

$$-\frac{1}{2}h'\delta g'_{tt}+\frac{1}{2}h'\delta g'_{xx}+\frac{1}{2}h'\delta g'_{yy}-\frac{k^2}{f}\delta A_t-\frac{k\omega}{f}\delta A_x+\delta A''_t=0$$

δA_x-variation equation:

$$\frac{k\omega}{f^2}\delta A_t+\frac{h'}{f}\delta g'_{tx}+\frac{\omega^2}{f^2}\delta A_x+\frac{f'}{f}\delta A'_x+\delta A''_x=0$$

$\delta\phi_x$-variation equation:

$$\frac{\left(\omega^2-3fk^2\right)}{f^2}\delta\phi_x-\frac{i\alpha\omega}{f^2}\delta g_{tx}+\frac{i\alpha k}{2f}\delta g_{tt}-\frac{3i\alpha k}{2f}\delta g_{xx}-\frac{i\alpha k}{2f}\delta g_{yy}+\left(\frac{f'}{f}+\frac{2}{z}\right)\delta\phi'_x+\delta\phi''_x=0$$

δg_{ty}-variation equation:

$$-\frac{\left(2zf'-6f+k^2z^2-Q^2z^4+8\alpha^6z^6+6\right)}{fz^2}\delta g_{ty}-\frac{12i\alpha^5\omega z^4}{f}\delta\phi_y-\frac{k\omega}{f}\delta g_{xy}-2Qz^2\delta A'_y-\frac{2}{z}\delta g'_{ty}+\delta g''_{ty}=0$$

δg_{xy}-variation equation:

$$\frac{k\omega}{f^2}\delta g_{ty}+\frac{\left(6f^2-f\left(-z^2f''+4zf'+Q^2z^4+20\alpha^6z^6+6\right)+\omega^2z^2\right)}{f^2z^2}\delta g_{xy}+\frac{12i\alpha^5kz^4}{f}\delta\phi_y+\left(\frac{f'}{f}-\frac{2}{z}\right)\delta g'_{xy}+\delta g''_{xy}=0$$

δA_y-variation equation:

$$\frac{\left(\omega^2-fk^2\right)}{f^2}\delta A_y-\frac{Q}{f}\delta g'_{ty}+\frac{f'}{f}\delta A'_y+\delta A''_y=0$$

$\delta\phi_y$-variation equation:

$$\frac{\left(\omega^2-fk^2\right)}{f^2}\delta\phi_y-\frac{i\alpha\omega}{f^2}\delta g_{ty}-\frac{i\alpha k}{f}\delta g_{xy}+\left(\frac{f'}{f}+\frac{2}{z}\right)\delta\phi'_y+\delta\phi''_y=0$$

A.5 Equations of motion: Magnetic fields

These are the perturbation equations of motion for the RN-metal in an external magnetic field.

δg_{tt}-variation equation:

$$\frac{\left(f\left(\mathcal{B}^2r^4-2r^2f''+2rf'-k^2r^2+4r^4Q^2-6\right)+6f^2+r^2\left(f'\right)^2\right)}{2f^2r^2}\delta g_{tt}$$
$$-\frac{\left(f\left(4\mathcal{B}^2r^4-r^2f''+4rf'+r^4Q^2+6\right)-6f^2+\omega^2r^2\right)}{2fr^2}\delta g_{xx}-\frac{f'}{4}\delta g'_{xx}$$
$$-\frac{\left(f\left(4\mathcal{B}^2r^4-r^2f''+4rf'+k^2r^2+r^4Q^2+6\right)-6f^2+\omega^2r^2\right)}{2fr^2}\delta g_{yy}$$
$$-3i\mathcal{B}kr^2\delta A_y-3r^2Q\delta A'_t-\frac{k\omega}{f}\delta g_{tx}-\frac{f'}{4}\delta g'_{yy}+\left(-\frac{f'}{2f}-\frac{2}{r}\right)\delta g'_{tt}+\delta g''_{tt}=0$$

δg_{tx}-variation equation:

$$\frac{\left(-\mathcal{B}^2r^4-2rf'+6f+r^4Q^2-6\right)}{fr^2}\delta g_{tx}+\frac{2i\mathcal{B}\omega r^2}{f}\delta A_y-2r^2Q\delta A'_x$$
$$+\frac{k\omega}{f}\delta g_{yy}-\frac{2}{r}\delta g'_{tx}+\delta g''_{tx}=0$$

δg_{ty}-variation equation:

$$-\frac{\left(\mathcal{B}^2r^4+2rf'-6f+k^2r^2-r^4Q^2+6\right)}{fr^2}\delta g_{ty}-\frac{2i\mathcal{B}kr^2}{f}\delta A_t-\frac{2i\mathcal{B}\omega r^2}{f}\delta A_x$$
$$-2r^2Q\delta A'_y-\frac{k\omega}{f}\delta g_{xy}-\frac{2}{r}\delta g'_{ty}+\delta g''_{ty}=0$$

δg_{xx}-variation equation:

$$\frac{\left(\mathcal{B}^2r^4-2rf'+6f+k^2r^2+2r^4Q^2-6\right)}{2f^2r^2}\delta g_{tt}$$
$$+\frac{\left(-f\left(2\mathcal{B}^2r^4-r^2f''+4rf'+r^4Q^2+6\right)+6f^2+\omega^2r^2\right)}{2f^2r^2}\delta g_{xx}$$
$$+\frac{\left(-6f^2+f\left(-r^2f''+4rf'-k^2r^2+r^4Q^2+6\right)-\omega^2r^2\right)}{2f^2r^2}\delta g_{yy}$$
$$-\frac{i\mathcal{B}kr^2}{f}\delta A_y-\frac{r^2Q}{f}\delta A'_t+\frac{k\omega}{f^2}\delta g_{tx}-\frac{f'}{4f}\delta g'_{yy}+\left(\frac{3f'}{4f}-\frac{2}{r}\right)\delta g'_{xx}+\delta g''_{xx}=0$$

δg_{xy}-variation equation:

$$\frac{\left(-f\left(\mathcal{B}^2r^4-r^2f''+4rf'+r^4Q^2+6\right)+6f^2+\omega^2r^2\right)}{f^2r^2}\delta g_{xy}$$
$$+\frac{k\omega}{f^2}\delta g_{ty}+\left(\frac{f'}{f}-\frac{2}{r}\right)\delta g'_{xy}+\delta g''_{xy}=0$$

δg_{yy}-variation equation:

$$\frac{\left(\mathcal{B}^2 r^4 - 2rf' + 6f - k^2 r^2 + 2r^4 Q^2 - 6\right)}{2f^2 r^2}\delta g_{tt}$$
$$+\frac{\left(-f\left(2\mathcal{B}^2 r^4 - r^2 f'' + 4rf' + k^2 r^2 + r^4 Q^2 + 6\right) + 6f^2 + \omega^2 r^2\right)}{2f^2 r^2}\delta g_{yy}$$
$$+\frac{\left(-6f^2 + f\left(-r^2 f'' + 4rf' + r^4 Q^2 + 6\right) - \omega^2 r^2\right)}{2f^2 r^2}\delta g_{xx}$$
$$-\frac{i\mathcal{B}kr^2}{f}\delta A_y - \frac{r^2 Q}{f}\delta A_t' - \frac{k\omega}{f^2}\delta g_{tx} - \frac{f'}{4f}\delta g_{xx}' + \left(\frac{3f'}{4f} - \frac{2}{r}\right)\delta g_{yy}' + \delta g_{yy}'' = 0$$

δA_t-variation equation:

$$\frac{i\mathcal{B}k}{f}\delta g_{ty} - \frac{Q}{2f}\delta g_{tt}' + \frac{Qf'}{2f^2}\delta g_{tt} - \frac{Q}{2}\delta g_{xx}' - \frac{Q}{2}\delta g_{yy}' - \frac{k^2}{f}\delta A_t - \frac{k\omega}{f}\delta A_x + \delta A_t'' = 0$$

δA_x-variation equation:

$$-\frac{i\mathcal{B}\omega}{f^2}\delta g_{ty} - \frac{Q}{f}\delta g_{tx}' + \frac{k\omega}{f^2}\delta A_t + \delta A_x'' + \frac{f'}{f}\delta A_x' + \frac{\omega^2}{f^2}\delta A_x = 0$$

δA_y-variation equation:

$$\frac{i\mathcal{B}k}{2f^2}\delta g_{tt} + \frac{i\mathcal{B}\omega}{f^2}\delta g_{tx} + \frac{i\mathcal{B}k}{2f}\delta g_{xx} + \frac{i\mathcal{B}k}{2f}\delta g_{yy} - \frac{Q}{f}\delta g_{ty}'$$
$$+\delta A_y'' + \frac{f'}{f}\delta A_y' + \frac{\left(\omega^2 - fk^2\right)}{f^2}\delta A_y = 0$$